An Exploration of 2D-LC-SERS:

A Novel Offline Detection Modality for Multidimensional Chromatography

By

Melanie Dawn Davidson

A Thesis Submitted to
Saint Mary's University, Halifax, Nova Scotia
In Partial Fulfilment of the Requirements for the Degree of
Masters of Science in Applied Science

April 2019, Halifax, Nova Scotia

Approved: Dr. Christa L. Brosseau
Supervisor

Approved: Dr. Clarissa Sit
Committee Member

Approved: Dr. Todd Ventura
Committee Member

Approved: Dr. Anthony Tong
External Examiner

Date: April 17, 2019

Abstract

An Exploration of 2D-LC-SERS:
A Novel Offline Detection Modality for Multidimensional Chromatography

By

Melanie Dawn Davidson

Multidimensional liquid chromatography (2D-LC) provides better resolving and separation power than conventional high-performance liquid chromatography (HPLC), and over the past decade has increasingly been applied in many different fields.[1] This thesis seeks to explore the extent to which surface-enhanced Raman spectroscopy (SERS) can be used as an offline detection modality for 2D-LC. This thesis hypothesizes that careful selection and modification of a three dimensional (3D) SERS substrate will be useful for characterization of fractions collected using 2D-LC. In particular, a mixture of four polyphenolic molecules was chosen for this proof-of-concept study. An optimised 2D-LC method was developed as part of this thesis. Various materials were evaluated as potential 3D-SERS substrates, with the most promising option being cellulose-based filter paper. Various modification strategies were explored to enhance the interaction between the polyphenolic molecules and the filter paper substrate. In the end, SERS-based detection of 2D-LC fractions proved challenging, even after optimization.

April 17, 2018

Acknowledgements

First and foremost, I would like to thank my supervisor Dr. Christa Brosseau for allowing me to complete my master's degree in her research group. I would not have been able to complete this degree without her, the academic, life guidance and support she has given me. I have had the honour to work in the Brosseau research group for the past 5 years as an undergraduate and graduate researcher, the experiences and friends I've made along the way will always stay with me. Thank you from the bottom of my heart for all you have done for me throughout the years and you will always be an important role model in my life.

I would like to thank my committee members Dr. Clarissa Sit, and Dr. Todd Ventura for their support and guidance through my degree. Also, Dr. Anthony Tong for being my external examiner and taking the time to review my thesis work.

Special thanks to all past and present Brosseau group members who have been a supportive family away from home. To Patricia Granados for all her help with LC and the new 2D-LC, as her help and expertise has been instrumental in my work. To Xiang Yang for help with SEM and imaging. Special thanks again to Alyssa Doue and the entire Saint Mary's University Chemistry Department for their help and support.

Lastly, I would like to thank my amazing friends and family who have helped me through this degree. Without all of you, I probably would not be writing this today. Thank you for lifting me up when I was down, and believing in me when I did not believe in myself. I can never express my gratitude enough.

I acknowledge the following agencies for funding: Faculty of Graduate Studies and Research, NSERC, and Canada Research Chairs.

List of Abbreviations

1D	One-Dimension
^{1}D	First Dimension
2D	Two-Dimension
^{2}D	Second Dimension
2D-LC	Two-Dimensional Liquid Chromatography
2D-LC-SERS	Two-Dimensional Liquid Chromatography with SERS Detection
3D	Three-Dimension
AgNP	Silver Nanoparticles
CM	Chemical Mechanism
DAD	Diode Array Detector
EC-SERS	Electrochemical Surface-Enhanced Raman Spectroscopy
EM	Electromagnetic Mechanism
FP	Filter Paper
GC	Gas Chromatography
HOMO	Highest Occupied Molecular Orbital
HPLC	High Performance Liquid Chromatography
HPLC-MS	High Performance Liquid Chromatography with MS Detection
HPLC-SERS	High Performance Liquid Chromatography with SERS Detection
LC	Liquid Chromatography
LC×LC	Comprehensive Multidimensional Liquid Chromatography
LC-LC	Heart-Cutting Multidimensional Liquid Chromatography
LSP	Localised Surface Plasmon
LSPR	Localised Surface Plasmon Resonance
LUMO	Lowest Unoccupied Molecular Orbital
mLC-LC	Multiple Heart-Cutting Multidimensional Liquid Chromatography
MS	Mass Spectrometry
NMR	Nuclear Magnetic Resonance
NP	Normal Phase
NPs	Nanoparticles
OCP	Open Circuit Potential
PSP	Propagating Surface Plasmon
PSPR	Propagating Surface Plasmon Resonance
Pyr	Pyridine
Pyz	Pyrazine
RP	Reverse Phase
SEM	Scanning Electron Microscopy
SERS	Surface-Enhanced Raman Spectroscopy
SP	Surface Plasmon
SPE	Screen-Printed Electrode
TLC	Thin Layer Chromatography
UHPLC	Ultra-High Performance Liquid Chromatography
UV-vis	Ultra-Violet Visible Spectroscopy

Table of Contents **Page #**

Chapter 4 Materials and Methods

Chapter 5 Results and Discussion

List of Figures

List of Tables

Chapter 1 Introduction

1.1 Preamble

Multidimensional liquid chromatography is an emerging technique in the field of analytical chemistry, with applications mainly in the areas of pharmaceutical, natural products, and food sciences due to sample complexity.[2] Alternatively, surface-enhanced Raman spectroscopy (SERS) has been in practice since the late 1970's as a sensitive and selective spectroscopic technique. SERS increasingly is coupled with chromatographic techniques as a detection modality due to its ability to detect small quantities, down to the single molecule level in a rapid and cost-effective manner. This thesis explores SERS as an offline detection modality for multidimensional liquid chromatography using separation and detection of polyphenols as a proof-of-concept example.

1.2 Objective of Thesis

Secondary plant metabolites, commonly found in fruits and vegetables, have been dominating the literature of food and nutritional sciences due to their potential health benefits.[3] Many have suggested that it is the antioxidant properties of polyphenolic compounds in particular that are the largest contributors to positive health benefits. However, the exact compounds and their varying combinations are still poorly understood due to the complexity of these biological samples and the sophisticated techniques required to examine them.[4]

Currently, the most widely used technique for the separation and detection of polyphenolic compounds is high-performance liquid chromatography (HPLC), with either mass spectrometry detection (HPLC-MS) or diode array detection (HPLC-DAD). Although liquid chromatography is powerful and highly sensitive, it begins to reach the end of its separation capacity for highly complex samples such as natural extracts, which

can contain thousands of metabolites, peptides, proteins and fatty acids.[2] Multidimensional liquid chromatography (2D-LC) is an emerging technique that addresses this issue due to the enhanced peak capacity allowing adequate separation of highly complex samples. For example, a few recent applications have employed 2D-LC to analyse and detect food pesticides, natural extracts for potential drug discovery, and detect impurities in pharmaceutical applications.[5–7]

Surface-enhanced Raman spectroscopy (SERS) has been recently applied as a detection modality for chromatographic techniques such as thin-layer chromatography (TLC), gas chromatography (GC), and HPLC due to its high sensitivity and selectivity.[8,9] As an alternative to expensive and complicated detectors such as mass spectrometry (MS) and nuclear magnetic resonance (NMR), SERS has become an attractive option.

This thesis hypothesizes that with sufficient optimization, SERS will be useful as an alternative offline detection modality for multidimensional liquid chromatography. To investigate this, the analysis will be optimized for a polyphenolic standard mixture for proof-of-concept work.

1.3 Scope of Thesis

This thesis consists of 6 chapters. Chapter 1 gives a brief introduction to the research conducted in this thesis, and highlights the major goal of this work. Chapter 2 provides a detailed literature review of the important aspects of this project including polyphenolic compounds, liquid chromatography, multidimensional liquid chromatography, surface-enhanced Raman spectroscopy and an introduction to 2D-LC-SERS. Chapter 3 provides a detailed description of the theory, which underlies the major experimental techniques used in this work including 1D and 2D liquid chromatography, Raman spectroscopy, SERS, and electrochemical SERS (EC-SERS). Chapter 4

summarizes the experimental procedures including a description of the electrochemical methods, preparation of filter paper substrates, and liquid chromatographic methodology. The major experimental results are presented in Chapter 5, which discusses the fabrication and characterization of various 3D-SERS substrates and the treatment and functionalization of these substrates before analyte detection. Chapter 5 also focuses on the characterization of four polyphenolic analytical standards: luteolin, quercetin, chlorogenic acid, and caffeic acid using Raman spectroscopy and SERS. The further characterization of these compounds using liquid chromatography and their separation using 2D-LC is also presented. Chapter 5 further presents the results for the new technique of 2D-LC-SERS. Chapter 6 summarizes the most important results obtained from this work and future work for this project is proposed.

Chapter 2: Literature Review

2.1 Introduction

The aim of this section is to provide an overview of naturally-occurring polyphenols and to discuss the importance of their detection in complex samples. This chapter then moves on to discuss both multidimensional liquid chromatography and surface-enhanced Raman spectroscopy, and highlights why a hyphenated 2D-LC-SERS technique may be of potential use for the separation and characterization of complex samples.

2.2 Polyphenolic Compounds

Natural products are a central subject at the interface between chemistry and biology, and are defined as molecules produced by a biological or "natural" source.[10] There is an increased interest in plant metabolites that are not only beneficial to the plant, but also to human health. Plant metabolites are generally divided into two major groups: primary and secondary plant metabolites.[11] Primary metabolites are compounds that play essential roles in plant life, including photosynthesis, respiration, growth, and development.[11] Included in this sub-group are acyl lipids, nucleotides, amino acids, and organic acids. All other phytochemicals fall into the sub-group of secondary plant metabolites. The compounds in this secondary group play key roles in protecting plants from herbivores and microbial infection, act as attractants to seed-dispersing and pollinating agents, provide UV protection, and function as signal molecules in the formation of nitrogen-fixing root nodules in legumes.[11–14]

Secondary metabolites have become an important area of research due to both the potential and demonstrated benefits to human health. This class of compounds has been shown to have positive outcomes in many areas including a possible role in prevention of

cancer, cardiovascular, neurodegenerative and infectious diseases, and osteoporosis.[3,4,12,13,15] The main theory regarding these benefits has been the antioxidant properties of these compounds, allowing them to act as radical scavengers and thereby reduce oxidative stress. In addition, they are good metal-chelating agents and remove potentially harmful and toxic metals from the body. [16–18]

Polyphenolic compounds are a group of secondary plant metabolites, that appear to hold promise for various human health concerns.[3,4,12,13,16,17,19] These molecules are classified based on their structure (one aromatic ring with one or more hydroxyl groups attached). Phenolic compounds are more popularly referred to as their sub-group, which are an even more specific group based on number and arrangement of carbon atoms in the molecular skeleton. Two common examples of these sub-groups are phenolic acids (skeleton: C6-C1) and flavonoids (skeleton: C6-C3-C6) (Figure 2.1) which contain some of the most investigated molecules of any polyphenolic compound group.[11]

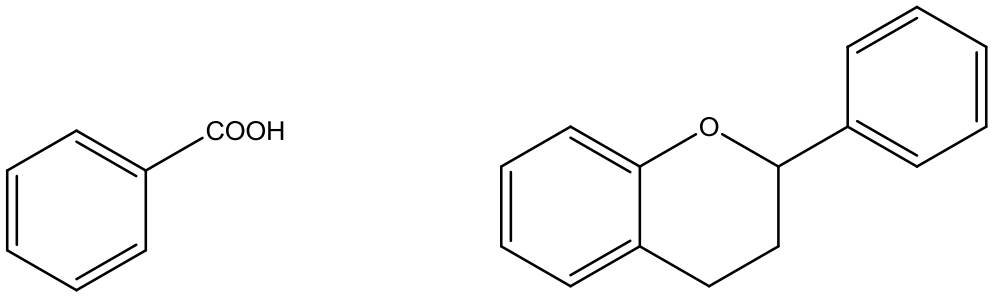

Phenolic Acid Flavonoid

Figure 2.1: Basic structures of phenolic acids and flavonoids

There have been more than 8,000 phenolic structures identified and reported throughout the plant kingdom and they are commonly found in vegetables, fruits, flowers and plant storage tissues.[4,11] The presence of these compounds in fruits and vegetables

provides high antioxidant potential and are a rich source of dietary antioxidants, including many different berries, apples, lettuce, kale, wines and teas.[12,13] Considering how beneficial polyphenols are to human health and their potential in reducing the impact of many diseases and afflictions, it has become an emergent research topic to understand the polyphenolic composition of these everyday foodstuffs and their specific roles as antioxidants.

The detection of these compounds is usually achieved with: capillary electrophoresis with Ultra-Violet (UV) or amperometric detection, quantum dots and metal nanoparticles, thin layer chromatography (TLC), as well as gas chromatography (GC) and high-performance liquid chromatography (HPLC) using UV or mass spectrometry (MS) detection.[14,16,20] HPLC-MS was first used in the detection of flavonoids in 1976, and has since then become the most commonly applied technique.[4,20,21] HPLC has emerged as a favoured technique due to its sensitive and reliable nature, especially with MS employed as a detector which can determine both molecular weight and structural features.[14]

2.3 Liquid Chromatography

Ultra-high performance liquid chromatography (UHPLC) and high-performance liquid chromatography (HPLC) are both common and powerful separation techniques that are currently the methods of choice for separations and analyses in many different fields, including biomedical chemistry, pharmaceuticals, forensics, and mircobiology.[22–27] The differentiation between the two being that UHPLC uses columns with much smaller particles sizes (< 2 µm) and thus requires higher pumping pressures to have solvent flow.[28] UHPLC was launched in the early 2000's and has helped overcome some issues in separation run time. The main components of UHPLC instrumentation include a mobile

phase, which is mixed and pushed through the system via a pump, the auto sampler, the column and the detector (Figure 2.2). The heart of this instrumentation is the column, where the analytical separation takes place.

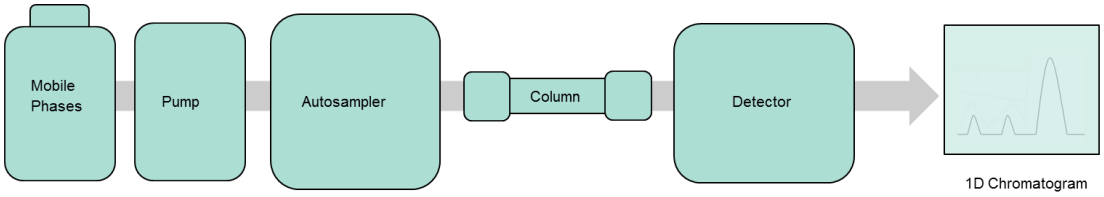

Figure 2.2: Schematic of UHPLC setup. (adapted from[2]).

Separation of mixtures is achieved based on the composition of the mixture being analysed, the mobile phases used and the column selected. UHPLC columns may be composed of different materials and can be tuned to give the best separation possible. The most widely used methods of chromatographic separations are normal phase (NP) and reversed phase (RP). NP chromatography uses a column packed with a highly polar stationary phase, such as silica, and a non-polar mobile phase solvents such as hexanes and isopropyl ether. RP chromatography uses a column with a non-polar stationary phase, such as C-18 or C-8 hydrocarbons, and highly polar mobile phase solvents, such as water, methanol, and acetonitrile.[29] In NP chromatography, the least polar components elute first, and increasing the polarity of the mobile phase will decrease the elution time. Conversely, in RP chromatography, the most polar components elute first, and increasing the polarity of the mobile phase will increase the elution time.[29] Reversed phase UHPLC is almost exclusively used in the separation of flavonoids due to the limited solubility of these compounds in typical NP solvents.[30] The use of UHPLC in the detection of flavonoids has been vast in the past ten years, with groups researching many different

samples including: tomatoes, cranberry and orange juices, wine, tea, chia seeds, and licorice.[30–37]

The separation and resolving power of UHPLC is limited to simple samples with moderate complexity.[1] Complex mixtures are most commonly encountered for natural or environmental samples as they can contain thousands of metabolites and other components such as peptides, proteins, and fatty acids that can occlude the ability of UHPLC to entirely separate out the mixture into definite components. The relevant biological samples that are most commonly being analysed for phenolic compounds are very complex in nature and can have co-eluting compounds, which limit accurate and precise results.

2.4 Multidimensional Liquid Chromatography

The introduction of multidimensional liquid chromatography aimed to overcome limitations, often outperforming conventional one dimensional ultra-high performance liquid chromatography (1D-UHPLC) for very complex samples.[2] Multidimensional liquid chromatography such as two-dimensional liquid chromatography (2D-LC) provides exceptional resolution compared to 1D UHPLC and is thus being increasingly explored for the analysis of complex samples.[30] Multidimensional or two-dimensional liquid chromatography (2D-LC) has been around in definition and theory since the 1980's.[38–40] However, due to a lack of understanding of the technique, and limited accessibility to adequate parts to build instrumentation, it was not until the past decade where this technique has entered mainstream research and become increasingly popular.[41]

The concept of multidimensional chromatography began with thin-layer chromatography (TLC) and a separation by two dimensions in space. By manually rotating the TLC plate after the initial separation and placing in it another solvent, the

separation could then continue based on another property. This basic concept has been adapted to fit other separation techniques, most popularly: gel electrophoresis, gas chromatography and liquid chromatography. Multidimensional separations offer greater separation and resolving power over conventional one-dimensional (1D) techniques. The basic instrumentational setup of 2D-LC is shown in Figure 2.3. Conventional separation is shown in blue; this illustrates the separation in the first dimension (^{1}D). Aliquots of the effluent from this separation (from the 1D column) are then passed through a second column, the second-dimension (2D) column. If the 2D column is to have a significant effect on the resolving or separation power of the technique, this column will have different separation selectivity.[2]

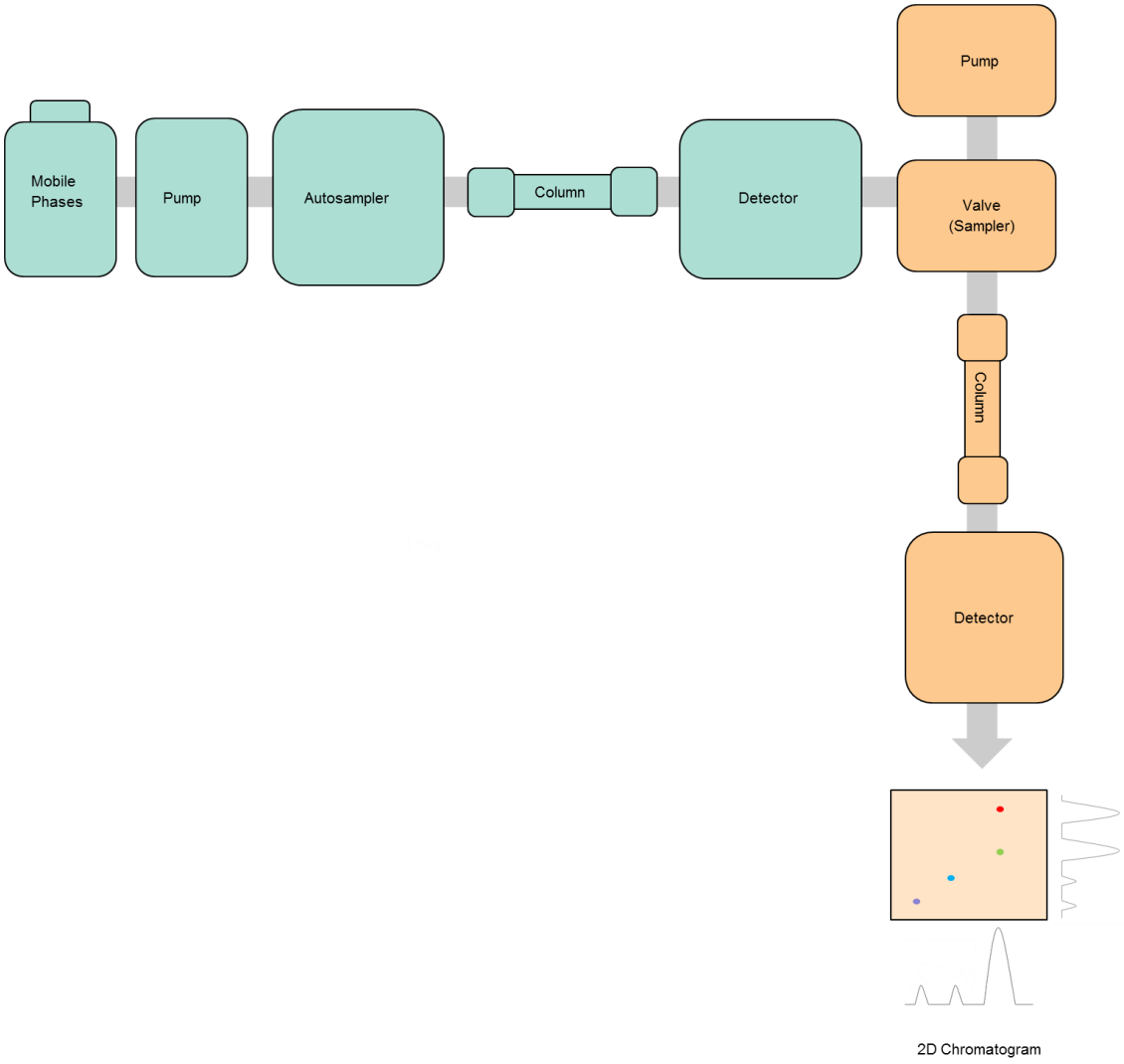

Figure 2.3: Schematic of 2D-LC setup (adapted from[2]).

Multidimensional liquid chromatography instrumentation can be run in two different ways: comprehensive (LC×LC) and heart-cutting (LC-LC), the pictorial difference is shown in Figure 2.4. Comprehensive is, as the name suggests, a more extensive analysis of a sample as the entirety of the sample that is run through the first dimension is transferred and analysed in the second dimension. This technique is most useful for gaining information on the entirety of a sample, which is usually exceedingly complex. However, because the whole of the 1D effluent is transferred to the second dimension, the run time of the second dimension needs to be increasingly fast in order to

analyse the entire sample. The heart-cutting technique takes the "heart" of peaks observed from the first dimension and transfers this portion of the sample to be analysed in the second dimension. Multiple heart-cutting (mLC-LC) is the term used when the sampling time allows and more than one sampling loop is available. This provides a more in-depth analysis of selected parts of the sample in the second dimension because of the less rigid time constraint with respect to the 2D analysis.

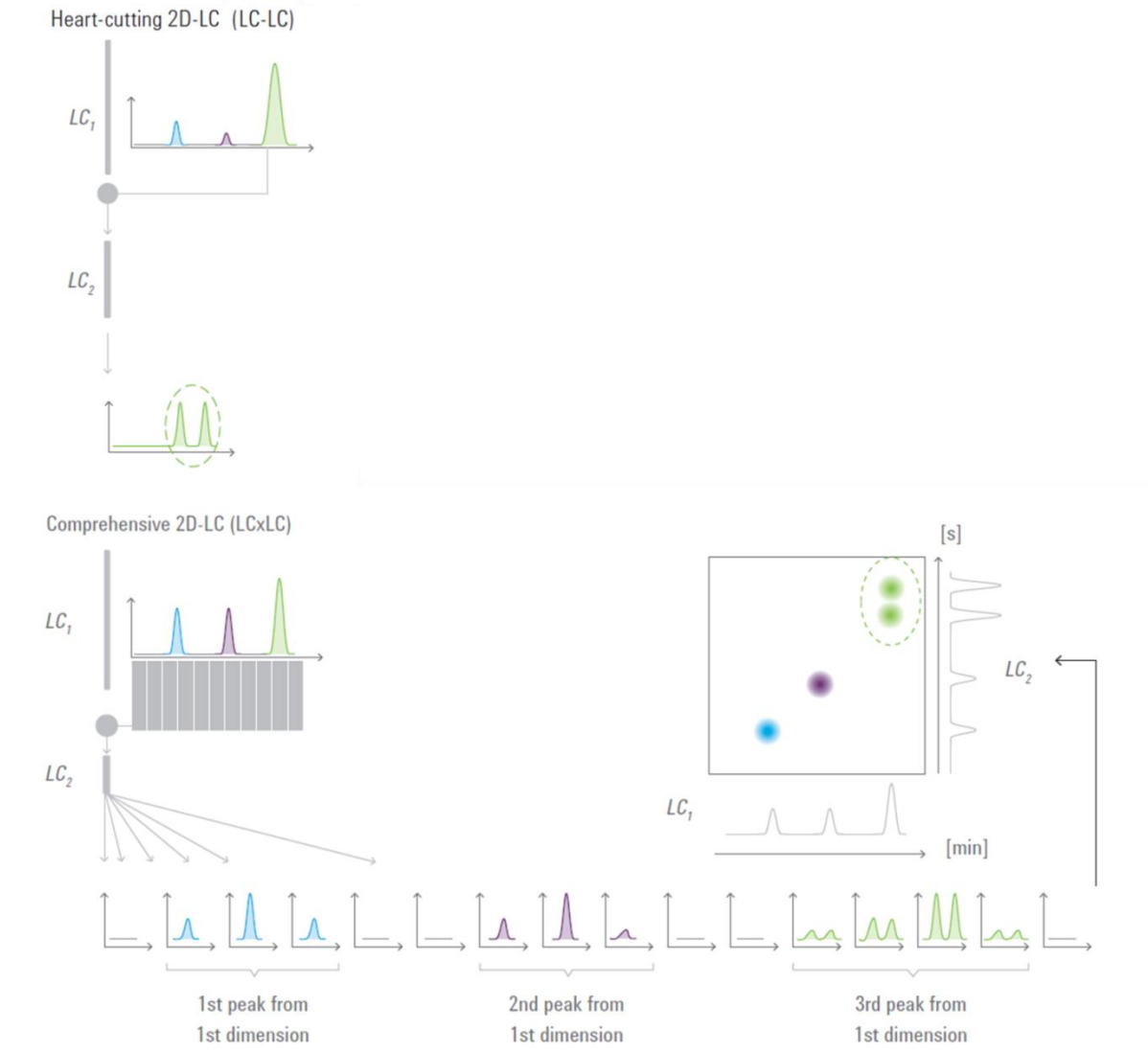

Figure 2.4: Conceptual representation of heart-cutting (LC-LC) and comprehensive (LC×LC) modes of 2D-LC (© Agilent Technologies, Inc. 2015. Reproduced with Permission, Courtesy of Agilent Technologies, Inc.)

It is easiest to explain the improvement in separation seen by 2D-LC over that of a single dimension separation through the concept of peak capacity. Peak capacity is the largest number of peaks that can be accommodated in the separation window in which all peaks are equally resolved.[2] This is a theoretical value as peaks never actually elute all equally resolved. In multidimensional separations, it is also important to consider the product rule in relation to peak capacities, the equation for which is shown below (equation 1.1).

$$n_{C,2D} = {}^{1}n_C \times {}^{2}n_C \qquad (1.1)$$

The peak capacity of two-dimensional liquid chromatography ($n_{C,2D}$) is equal to the product of the peak capacities from the first dimension ($^{1}n_C$) and the second dimension ($^{2}n_C$). This is a great improvement over tandem LC (where the effluent flows from one column directly into the other) where the best overall achievable peak capacity is the sum of the values from each dimension.[42]

The visualization of this concept can be seen in Figure 2.5, and through the following analogy: the peak capacity of the ^{1}D separation can be equated to parking cars along the side of the road, where as the peak capacity of the ^{2}D separation can be equated to parking cars in a parking lot. Obviously, many more cars can be accommodated in the parking lot compared to the road.

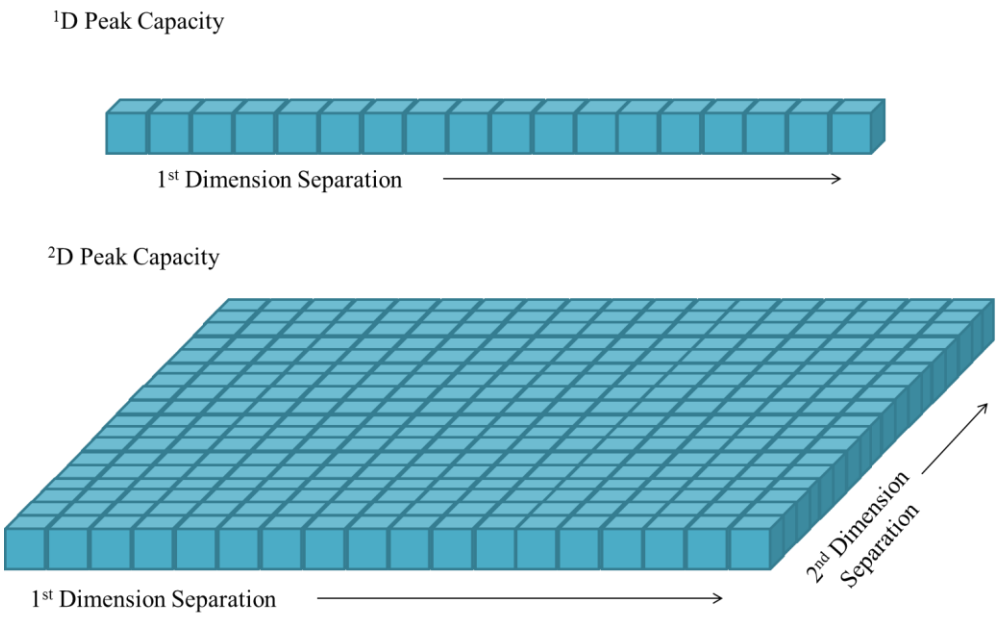

Figure 2.5: Schematic representation of peak capacity in one and two dimensions (adapted from[2]).

Over the past 30 years researchers began constructing their own instruments to practically explore 2D-LC theory that had been proposed in the 1980's.[43] Thus began a growth in chromatographic exploration of samples that had previously been too complex or difficult to resolve using conventional 1D separation methods. However, it has only been in the past five years that multidimensional liquid chromatographic instruments have been commercially available and thus have been able to reach the general researcher who does not have the expertise or time and resources to build their own instrumentation. In these recent times the most popular uses for this instrumentation has been in the analysis of pharmaceuticals and natural products.[2] Some recent examples of flavonoid-containing samples which have been analysed using 2D-LC include herbal medicines, green and black tea, and grape seeds.[30,44–46]

2.5 Surface-Enhanced Raman Spectroscopy (SERS)

Surface-enhanced Raman Spectroscopy (SERS) was first developed in the 1970's when it was shown that adding a layer of nanoscale, noble metal to a surface increased the Raman spectral intensity a million fold.[47–49] This technique has since proven to be useful in the detection of very dilute samples due to the sensitivity of Raman spectroscopy and the significant quenching of fluorescence by the metal nanoparticles that can normally hinder the Raman signal.[50,51] This spectroscopic technique has been used in various applications in which selectivity and sensitivity are extremely important and where there exist large consequences for inaccurate results, including drug discovery, forensic analysis, and homeland security.[52] As a result of these advantages and the lack of spectral interference from solvents such as water, several studies have used SERS as a detection modality for different chromatographic techniques.

SERS was first used as a detection modality in conjunction with thin-layer chromatography (TLC) in 1977 by Henzel *et al*.[50] Since then, it has been used to detect synthetic dyes, drugs in botanical dietary supplements, and tobacco-related biomarkers in urine.[50,53,54] In these studies, silver colloid can be added to the TLC plate and SERS conducted directly on the plate.[50,53] In others, the sample and support are removed from the TLC plate and eluted with a different solvent before being added to a sample of silver nanoparticles (AgNP) and SERS was subsequently conducted using a quartz cuvette.[54] Both approaches were shown to be sensitive and selective, with results produced using short detection times and simple sample pre-treatment strategies.

SERS has also been shown to be a useful detector in combination with gas chromatography (GC). One study deposited eluents from the GC-column onto a TLC plate pre-treated with Ag colloid, and another adsorbed eluents onto a modified silver foil

surface.[55,56] Another method also condensed the analyte on a moving, liquid-nitrogen-cooled ZnSe window, which had a 5 nm thick layer of Ag formed using physical vapour deposition.[52] These studies all successfully coupled SERS with GC to provide sensitive and selective methods of molecular detection. In the latter study, detection limits lower than those of GC coupled with mass spectrometry (GC-MS) were reported.

Many studies have reported the use of SERS as a detector for HPLC and UHPLC. The two main ways of interfacing these two technologies are referred to as online and offline.[8] Online specifies at-line instrumentation that collects SERS spectra in real time as eluents are coming off the column. Some of the main methods to accomplish online HPLC-SERS have been to introduce nanoparticles to the mobile phase flow, or the reuse of a roughened electrode placed at the end of the column.[8] However, online SERS detection of analytes as they elute from the column can be problematic. By adding colloid to the mobile phase and allowing it to aggregate, there are risks of the colloid sticking to the inside of flow cells used to collect the online SERS spectra and thus requiring it to be cleaned between samples. There are also memory effects when using the roughened electrodes as they are also required to be cleaned between samples to ensure accurate and reproducible SERS signals. One attempt to overcome this memory effect has been to apply sheath-flow SERS; however, this requires a fairly complex home-built setup.[9,57]

Offline analysis is a slightly more labour intensive method as the eluents must first be collected and SERS spectra then obtained using separate Raman instrumentation. This methodology removes the time-critical element of the analysis and thus care in optimizing the SERS conditions for each fraction independently can be taken into account.[8,58] As a result of not needing to compromise SERS response for separation efficiency, a potentially more relevant and accurate SERS signal can be achieved.

2.6 Three-Dimensional Surface-Enhanced Raman Spectroscopy Substrates

SERS has proven to be a highly sensitive and selective spectroscopic technique.[51] A key contribution to the enhancement of the SERS signal comes from the physical structure of the SERS active substrates. Various types of substrates have been developed, however paper-based substrates have been some of the most notable.[59] Advantages over more conventional substrates such as glass or silicon-based substrates are due to the high packing density and uniform distribution of the nanoparticles formed within the paper-based substrates. Different paper-based materials have been used for the fabrication of SERS substrates such as blotting paper, cardboard, printing paper, newspaper, and most commonly laboratory filter paper. Filter papers have been popular due to their large availability, flexibility, biodegradability, and low cost.[59,60]

Central to the SERS enhancement mechanism is the creation of SERS active "hot spots".[59,60] "Hot spots" are places where the local electric field is exceptionally intense and arises from regular spacing between nanoparticles on the substrate.[61,62] Nanoparticles self-assemble on the substrate and thus a 3D substrate can accommodate many more hot spots than planar (2D) substrates.[61] Silver nanoparticles in particular prefer to be loaded on a filter paper substrate due to their interaction with the hydroxyl groups on the surface of the paper fibers.[59] Paper-based substrates and filter paper especially are a sensitive, cost-effective, and reproducible alternative to conventional SERS substrates.

2.7 Multidimensional Liquid Chromatography with Surface-Enhanced Raman Spectroscopy

This thesis work will apply the principle of offline UHPLC-SERS to multidimensional liquid chromatography. To the knowledge of the author, this is the first time SERS will be explored as a detection modality for 2D-LC. Since this is still an

emerging chromatographic technique with potentially extensive and beneficial outcomes, exploring the coupling of 2D-LC and SERS could become very meaningful.

Advantages of the use of SERS over a more standardized detection modality like MS include the straightforward signal acquisition and reduced cost. SERS is sensitive to the structure of the molecule and can thus differentiate between structural isomers whereas MS relies on mass-to-charge ratios and proves challenging for the detection of isomers and also poorly ionizing molecules.[9,57] MS techniques also need to be performed in vacuum and thus it can be difficult to interface with samples and solvents from LC.[55] Most importantly, SERS is comparably sensitive and selective to MS and can detect molecules at very low levels, even down to the single molecule detection regime.[57]

Chapter 3: Theory

3.1 Introduction

This section provides the necessary theoretical background for concepts central to this thesis work as well as an introduction to the instrumentation used in this project. This chapter starts with a focus on liquid chromatography in general, and then moves on to concepts related to multidimensional liquid chromatography and the theory behind this technology. The fundamentals of plasmonics is then discussed as it relates to the SERS enhancement phenomenon, with a focus on metal nanospheres, most importantly silver. Finally, the theory behind the instrumentation of Raman spectroscopy, surface-enhanced Raman spectroscopy and electrochemical surface-enhanced Raman spectroscopy are all discussed.

3.2 Liquid Chromatography

Chromatography is a separation process in which a sample is distributed between two phases in the chromatographic column.[63] These two phases are the stationary phase and the mobile phase. The stationary phase is as the name suggests, stationary and is either solid, porous, or surface-active materials in small-particle form or a thin film of liquid coated on a solid support or a column wall.[63] The mobile phase is either a gas or a liquid, which transports the analyte through the chromatographic column. In the context of this work the mobile phase is a liquid and thus the chromatographic method is referred to as liquid chromatography.

The goal of chromatography is to completely separate all components of a sample in the shortest time possible.[64] In order to achieve this goal, different parameters of the separation can be optimized, such as the composition of mobile and/or stationary phases and the variation of the mobile phase flow rate. A simple chromatogram is depicted in

Figure 3.1. In this example, the sample is injected into the system at t = 0s, and the non-retained species will elute at retention time (t_0), which corresponds to the flow rate of the mobile phase. Compounds A and B each interact with the stationary phase differently and thus elute later and at different times, t_R(A) and t_R(B). The width of each peak (w) is defined as the intersection of the tangents on each side of the peak with the baseline.[64] These parameters can be used to derive other parameters to express the quality of the separation and quantify the components.

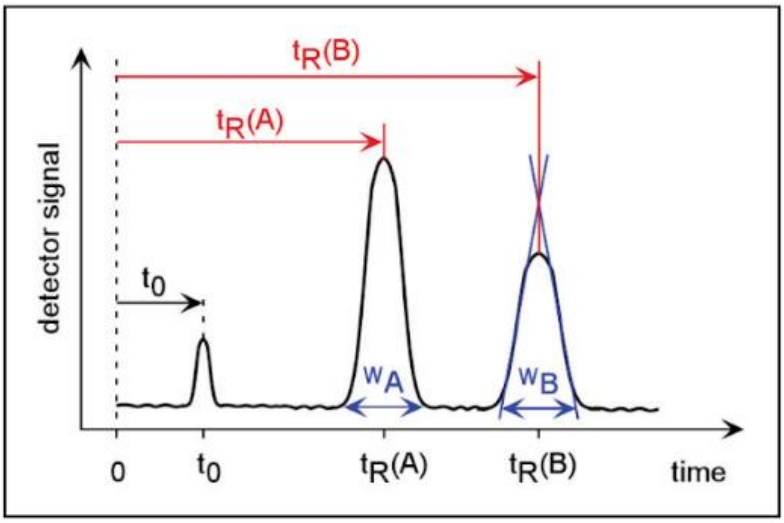

Figure 3.1: Simple chromatogram depicting retention time, t_R, and peak width, w. (Reproduced with permission from Manz, A.; Dittrich, P. S.; Pamme, N.; Iossifidis, D. *Bioanalytical Chemistry: Second Edition*. Copyright 2015 Imperial College Press.)

A few of the most important principles in chromatography include the capacity factor, the selectivity factor, and band broadening. The capacity factor (k') describes the velocity of the analyte relative to the velocity of the mobile phase and can be defined by equation 3.1. If k' is much smaller than 1, the analyte moves too quickly and the elution time is too short to determine an exact retention time.[64]

$$k' = \frac{t_R - t_0}{t_0} \tag{3.1}$$

The selectivity factor (α) describes the relative velocities of analytes with respect to each other and is described in equation 3.2. This factor details how well a chromatographic method can distinguish between two analytes.[64]

$$\alpha = \frac{k'_B}{k'_A} = \frac{t_R(B) - t_0}{t_R(A) - t_0} \quad (3.2)$$

The efficiency of a chromatographic separation is dependent on band broadening. If band broadening is large, there can be peak overlap (co-elution) and thus resolution will be diminished. Band broadening for a column with length (L) is quantitatively expressed with the concept of height equivalent to a theoretical plate (H), or plate number (N).[64] The larger the number of plates (N), and the smaller the plate height (H), the better the chromatographic efficiency will be.[64] The parameters which influence band broadening are highlighted in the van Deemter equation (3.3),

$$H = A + \frac{B}{u} + C \cdot u \quad (3.2)$$

where A, the Eddy diffusion or multipath term, describes the influence of column packing on band broadening. This term is constant for a given column and is independent of flow rate. The second term, B/u, describes the diffusion in or opposed to the direction of flow. The B/u term is also called the longitudinal diffusion term and is inversely proportional to the flow rate (u). The third term, C·u, describes the resistance to mass transfer between the stationary phase and mobile phase, and is directly proportional to flow rate. The optimum flow rate for a chromatographic separation can be determined by plotting H as a function of u, as seen in Figure 3.2.

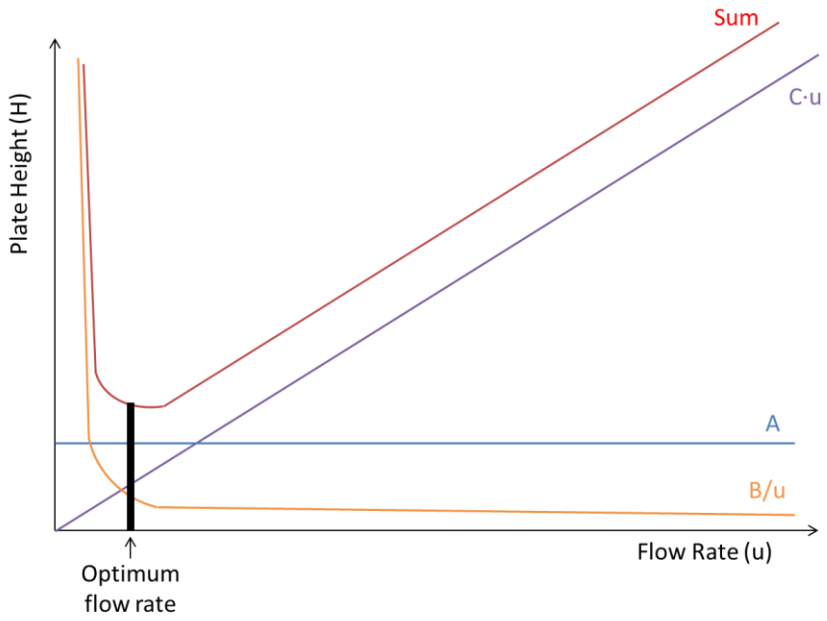

Figure 3.2: A van Deemter plot for the determination of optimum chromatographic flow rate

3.3 Multidimensional Liquid Chromatography

Multidimensional liquid chromatography was introduced in order to combat separation inadequacies in the single dimension. These main short comings arise for either intensely complex samples or samples that contain one or more pairs of compounds that are difficult to resolve.[1,65] An example of a highly complex sample is a natural, biological extract, which can be comprised of thousands of metabolites and other compounds. These samples are too complex to be adequately separated in one dimension and co-elution and peak overlap often result. Difficult to resolve compounds are those that contain compounds such as enantiomers (with the use of a chiral column) or chemically similar compounds that would be difficult to distinguish from each other. Multidimensional chromatography is an advantageous tool in these instances as the increased peak capacity allows for increased and improved separation power. Even though the separation power is greatly increased for 2D-LC, it is not always the best

technique for every separation. Since this technique uses multiple dimensions, the instrumentation and processing becomes much more intricate and thus expensive, it is also time consuming and requires additional training and expertise. A sample should not be chosen for multidimensional separation if it can be adequately separated in a reasonable time using single dimension chromatography.

The height of the instrumental intricacy and the heart of the multidimensional separation is the ^{2}D switching valve. In 2D-LC, the desired ^{1}D effluent(s) is/are captured and temporarily stored in a sample loop until being transferred to the ^{2}D column for further separation. This is all done within the ^{2}D switching valve. A schematic of the valve and the switching positions for LC-LC are shown in Figure 3.3. In this image the blue line indicates the tubing that connects the ^{1}D column to the valve and then to waste. The red line is the tubing connecting the ^{2}D pump to the valve and then onto the ^{2}D column. It is seen that between ports 4 and 5 that there is a sample loop, this loop is where the ^{1}D effluent is temporarily stored until transferred to the ^{2}D-column. In the case of instrumentation that is able to carry out multiple heart-cutting (mLC-LC) separations, there are many loops available for temporary storage of desired cuts. The instrument used for this project is equipped with two decks, each containing 5 sample loops. While keeping one loop in each deck open for continuous flow, there is the option to store 8 ^{1}D cuts at any one time. The top valve image shows the position which allows for the storage of effluent into the loop, while the second image shows the valve position for the effluent to be transferred to the ^{2}D column.

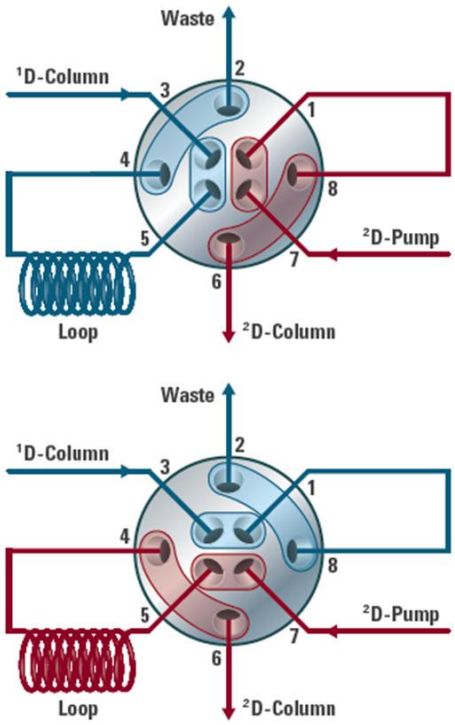

Figure 3.3: Configurations of an 8-port/2-position valve needed for LC-LC separation (© Agilent Technologies, Inc. 2015. Reproduced with Permission, Courtesy of Agilent Technologies, Inc.)

An important topic for discussion when considering 2D-LC is orthogonality between the two dimensions. For ideal multidimensional separation, the second dimension would be as dissimilar as possible or uncorrelated. Having two uncorrelated systems would provide the best chance of separation in the ^{2}D. An example of that would be using either NP or RP separation in the 1D, followed by whichever is unused in the 2D. This type of separation can be seen graphically in Figure 3.4 (C). However, this is not usually possible due to solvent miscibility issues when switching from one solvent system to another between dimensions. The most probable situation for real world samples can be seen in Figure 3.4 (B). There is some orthogonality, but more correlation than in 3.4 (C). This also shows some areas of the chromatogram with a higher density of peaks than others, which is relevant in fields such as the pharmaceutical industry. The worst case

scenario is shown in Figure 3.4 (A) where the separation in both dimensions is highly complementary. This would suggest that any co-eluting peaks in the ^{1}D would also co-elute in the ^{2}D, thus making the ^{2}D separation redundant.

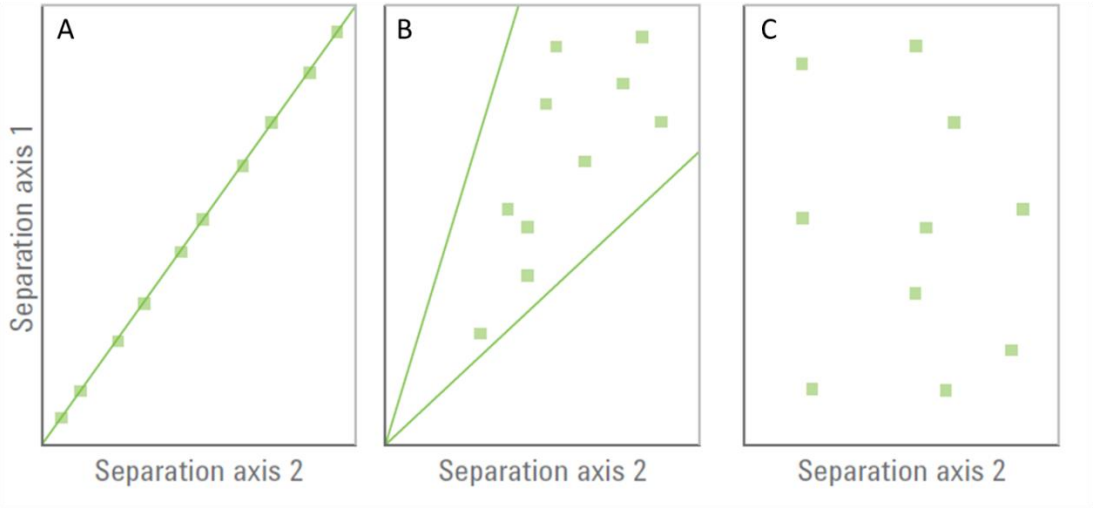

Figure 3.4: Effects of different degrees of correlation of separation mechanisms in plots of first versus second dimension retention. (A) Example of separations with total correlation; (B) example of separations with partial correlation; (C) example of orthogonal separations. (© Agilent Technologies, Inc. 2015. Reproduced with Permission, Courtesy of Agilent Technologies, Inc.)

3.4 Surface-Enhanced Raman Spectroscopy

3.4.1 Plasmonics

At the nanoscale, metals show different physical behaviours resulting in unique electrical and optical responses.[66] Some of the oldest and most notable examples include the embedding of colloidal metal nanoparticles into glass works to create differing colours, more commonly known as stained glass. Plasmonics is the field of research which explores these unique interactions between certain nanoscale metals and incident light. At the nanoscale, metals can convert incident light into localised electric fields, which is made possible by the strong interaction between the oscillating electric field of the light and the free electrons in the nanostructures.[67] The metal is a key component to

plasmonics as it is the material which supports the surface plasmons (SPs), which are the electromagnetic waves coupled to the collective oscillation of free electrons in the metal.[66,67]

Surface plasmons can be classified as one of two types: localized surface plasmon (LSP), or propagating surface plasmons (PSP). LSPs are described in metals that are nanoscale in all dimensions, such as a nanosphere. Contrarily, PSPs are described in metals that are nanoscale in one or two dimensions, such as a nanofilm or a nanowire respectively.[66,67] Both LSPs and PSPs give rise to resonance, accurately named localized surface plasmon resonance (LSPR) and propagating surface plasmon resonance (PSPR), respectively. This thesis deals only with LSPs and LSPR as it pertains to the research objective.

LSPR can most easily be described using Mie theory, which defines the extinction (extinction = scattering + absorption) spectra of spherical particles as shown in equation 3.3.[67,68] This equation solves for C_{ext}, which is the extinction cross-section, ε_m is the complex dielectric function for the metal which includes both a real (ε_r) and an imaginary component (ε_i), R is the radius of the spherical nanoparticle, and λ is the excitation wavelength. The dielectric function of a material varies with changing excitation wavelength of light, as it expresses the unique interaction between that material's electrons and the incident light.[67]

$$C_{ext} = \frac{24\pi^2 R^3 {\varepsilon_m}^{3/2}}{\lambda}\left[\frac{\varepsilon_i}{(\varepsilon_r+2\varepsilon_m)^2+{\varepsilon_i}^2}\right] \quad (3.3)$$

Since the interaction of light and a metal nanoparticle is highly dependent on its dielectric properties, ε_r and ε_i , when the denominator in the bracketed portion of the equation approaches zero, C_{ext} will become very large and its optical absorption and scattering

becomes very strong, which is known as the resonance condition.[67] To achieve this condition a material with a large, negative real component, and a small, positive imaginary component of the complex dielectric function is required.[67] This is in general only possible for metals, and only reigns true for some metals, such as Ag, and Au, as shown in Figure 3.5 which compares the dielectric constants of Ag and Au to those of Si.

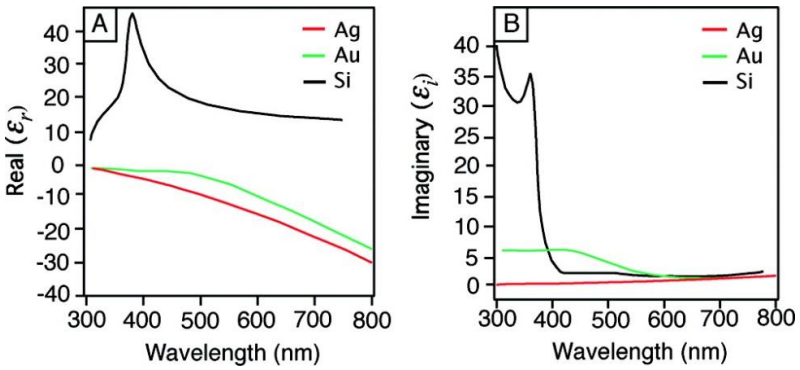

Figure 3.5: Plots of the real (A) and imaginary (B) components of the dielectric function of Ag, Au, and Si (Reproduced with permission from Rycenga, M.; Cobley, C. M.; Zeng, J.; Li, W.; Moran, C. H.; Zhang, Q.; Qin, D.; Xia, Y. *Chem. Rev.* **2011**, *111* (6), 3669–3712. Copyright 2011 American Chemical Society.)

The SP strength can then be determined by using equation 3.4 through the quality factor (Q).

$$Q = \frac{w(d\varepsilon_r/dw)}{2(\varepsilon_i)^2} \tag{3.4}$$

The SP strength is directly proportional to Q, therefore large Q values mean strong surface plasmons and small values mean weak SPs. Generally, for plasmonic applications, the Q value should be greater than 10 in order to have strong enough SPs. The quality factors of varying metals are plotted and compared in Figure 3.6. Ag displays the most useful plasmonic behaviour as it has the highest Q factor over the longest range. Au and Cu are also good but suffer from d-band interference below ~600 nm.[67] Lithium is

also potentially useful, but practical use is limited due to reactivity. Hence, this work uses only Ag nanomaterials as it is the most widely applicable and most used metal for SERS applications, which is a main objective of this thesis work.

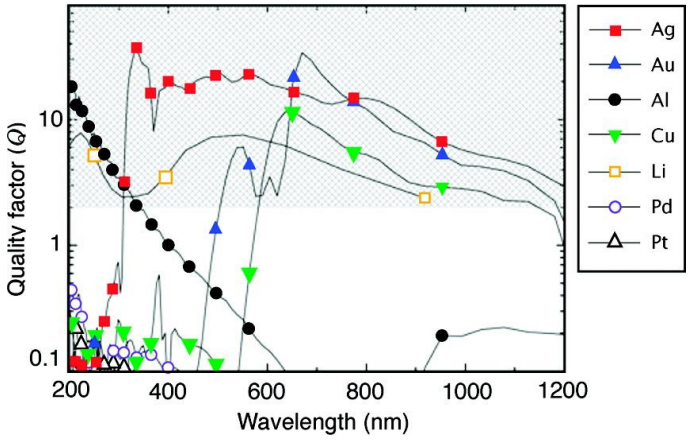

Figure 3.6: Quality factor (Q) of the LSPR for a metal/air interface of various metals. The shaded area represents the area of interest for many plasmonic applications (Reproduced with permission from Rycenga, M.; Cobley, C. M.; Zeng, J.; Li, W.; Moran, C. H.; Zhang, Q.; Qin, D.; Xia, Y. *Chem. Rev.* **2011**, *111* (6), 3669–3712. Copyright 2011 American Chemical Society.)

3.4.2 Raman Spectroscopy

Raman spectroscopy is a common vibrational technique that is based on the inelastic scattering of monochromatic light.[69,70] Light can interact with matter in one of three ways; the photons that make up the light may be absorbed, transmitted or scattered by atoms and molecules. Most of the scattered light has the same wavelength as the incident light, this is known as elastic or Rayleigh scattering. However, a small fraction of the incident photons are shifted in wavelength by molecular vibrations and rotations of the molecules in the sample, these shifts are either known as Stokes or anti-Stokes scattering.[69,70] Both Stokes and anti-Stokes scattering are forms of inelastic scattering, called Raman scattering. The Stokes and anti-Stokes scattering and their shifts in energy are shown in Figure 3.7. As described above, Rayleigh scattering has the excited

molecule returning back to its ground state with no net energy transfer, and therefore does not contain any vibrational information. Stokes and anti-Stokes scattering, which are collectively known as Raman scattering, undergo a net energy loss and gain respectively. In most cases molecules are present in the ground electronic state; therefore the Stokes Raman scattering is more probable and thus more intense. The spectrum of this wavelength shifted light is known as the Raman spectrum.[69,70] Raman spectra usually contain sharp bands that are characteristic of the specific vibrational modes of molecules in the samples, sometimes referred to as chemical 'fingerprints' and therefore can be used as a means of identification. The intensity of the spectra is proportional to concentration as well, and as a result Raman spectra can also be used for quantitative analysis.[69,70] However, since only one in every 10^6-10^8 photons are Raman scattered, it is an inherently weak process. As a result, Raman spectroscopy has historically only been useful in the analysis of bulk powders and neat liquids, due to this lack of sensitivity. However, this process can be greatly enhanced, up to 10^4 -10^{11} orders of magnitude, by using a technique known as surface enhanced Raman spectroscopy (SERS).[47,51,71]

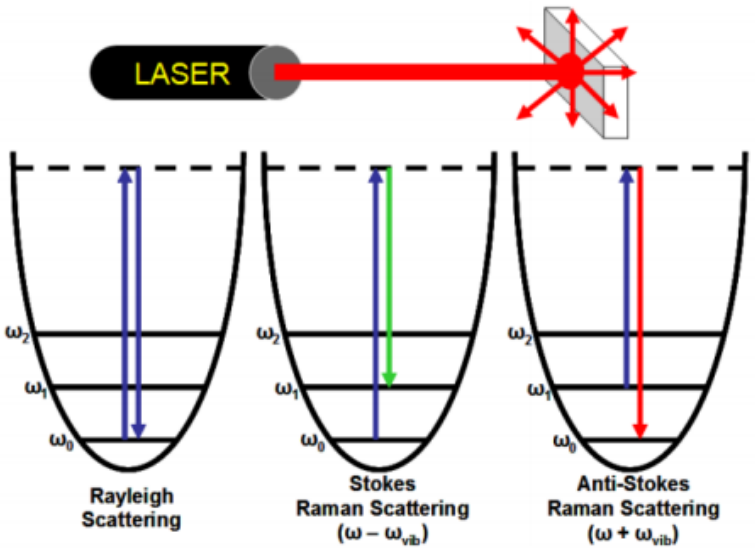

Figure 3.7: Diagram which shows the different light scattering modes: Rayleigh, Stokes, and anti-Stokes scattering.

3.4.3 Surface-Enhanced Raman Spectroscopy

In 1974 the enhanced Raman spectrum of pyridine adsorbed on a roughened silver electrode was reported.[48] Authors originally believed that this improvement was due to increased surface area and thus coined the term surface-enhanced Raman spectroscopy (SERS).[72] However in 1978 this idea was challenged; Creighton & Albrecht[49] attributed the enhancement to a chemical or charge-transfer effect and Jeanmaire & Van Duyne[47] to an electromagnetic effect.[72] In more recent years, the fundamental ideas concerning the origin of the SERS signal have been extensively studied and continue to evolve. Generally, there is a consensus on the contributions to the enhancement, which still involves both a chemical (charge-transfer) mechanism as well as an electromagnetic mechanism based on the presence of the localized surface plasmon resonance.[67,72]

The chemical SERS enhancement is thought to arise from electron transfer between the molecule and the nanoparticle. This is driven by the incident radiation which facilitates the excitation of electrons from the HOMO to the LUMO in the molecule.[67] However, the chemical mechanism (CM) is thought to only contribute $10\text{-}10^2$ to the overall enhancement.[67,71] The electromagnetic SERS enhancement arises due to LSPR modes, which can focus light into nanosized volumes, drastically increasing the electric field intensity near the nanoparticle, which can then be scattered by molecules on or in the vicinity of the metal surface.[67] Theoretical predictions suggest that the electromagnetic mechanism (EM) contributes the most to SERS, approximately $10^4\text{-}10^{10}$. Combining both the CM and EM contributions, one can see that the Raman signal for a desired analyte can be increased by $10^5\text{-}10^{12}$ times simply by incorporating metal nanoparticles into the system. This level of signal enhancement makes single molecule detection a possibility, as has been illustrated for certain systems.[67,72]

The EM enhancement, and therefore the SERS enhancement, sharply decreases as the distance between the analyte and the nanoparticle surface increases.[71,73] The EM enhancements for SERS has been derived to be $1 / r^{10}$ due to the decay length of the LSPR. However, the $1/ r^{10}$ dependence is theoretical and is highly susceptible to the differing shapes and sizes of nanoparticles on the surface.[73] To fully benefit from the overall SERS enhancement it has been experimentally determined that molecules should be within 2 – 4 nm of the nanoscale roughened surface.[71] To achieve this very close proximity, molecules that have a low affinity for the metal surface have been coaxed closer to the surface by using self-assembled monolayers, aptamers, and other surface treatments of attractive nature to the analyte in question.[71]

3.4.4 Electrochemical Surface-Enhanced Raman Spectroscopy

Electrochemistry is a branch of physical chemistry that is focused on the interaction between electrical and chemical changes in a system. This technique has become popular in analytical fields for its application in environmental monitoring, industrial quality control, and biomedical analysis.[74] In contrast to many homogenous bulk solutions, electrochemical processes take place at the electrode-solution interface. There are two main types of electroanalytical measurements: potentiometric and potentiostatic, the difference between the techniques being the type of electrical signal used for quantification.[74,75] Both types require an electrochemical cell. The cell is comprised of at least two electrodes (conductors) and an electrolytic solution. The electrolytic solution is commonly an aqueous salt solution; however choice of solvent is dependent on analyte solubility and its redox activity. The solvent should also not react with the analyte or any potential products, and should not undergo electrochemical reactions over a wide potential range.[74,75]

This thesis work uses potentiostatic measurements, which focus on the charge-transfer process at the electrode-solution interface. Using this methodology, the electrode potential is being used to drive an electron transfer reaction and the resulting current is measured.[74] Potentiostatic measurements use a three-electrode configuration, which consists of a working, reference, and counter electrode. The working electrode is where the reaction of interest takes place. The reference electrode provides a reproducible potential independent of the sample composition in which the working electrode potential is compared. The counter electrode is an inert conductive material such as platinum or graphite.[74]

Coupling SERS and electrochemistry is termed electrochemical surface-enhanced Raman spectroscopy (EC-SERS). This technique allows for the detection of analyte molecules on a metallic surface at a chosen applied voltage. EC-SERS can be useful to detect signal of an analyte in biologically relevant electrical environments and to monitor surface redox processes.[47,51] Application of a voltage also changes the chemical and electrical environment and can change the position or conformation of the molecule on the surface. This technique can be exploited to obtain a desired conformation or oxidation state of the analyte molecule while using the selective and sensitive SERS technique.[47]

Chapter 4: Materials and Methods

4.1 Introduction

This section starts with a description of the reagents used in this thesis work. The instrumentation is then noted with the corresponding procedures and rationale. Finally the methodology for SERS substrate fabrication and their characterization is outlined.

4.2 Reagents

$AgNO_3$ (99.9999%), $NaBH_4$ (≥96%), NaCl (99%), KCl (≥99%), and pyridine (≥99%) were all purchased from Sigma Aldrich (St, Louis, MO, USA). Citric acid (>99%) was purchased from Alfa Aesar (Tweksbury, MA, USA) and sodium citrate from ACP (Montreal, Quebec). Chromatographic analytical standards of luteolin (95%), quercetin dehydrate (96%), caffeic acid (98%) and chlorogenic acid (96%) were purchased from Toronto Research Chemicals (TRC) Canada (Toronto, Ontario). All chemicals were used without further purification and all solutions were prepared using Millipore water (≥ 18.2 MΩ•cm). All glassware was placed in an acid bath composed of neat H_2SO_4 overnight, and was then thoroughly rinsed with Millipore water prior to use.

4.3 Instrumentation

4.3.1 Spectroscopy

4.3.1.1 UV-vis Spectroscopy

UV-visible measurements were obtained using a Cary 60 UV-visible spectrometer (Agilent, Santa Clara, CA). This instrument was used to record UV-vis absorbance measurements for the analyte to select wavelengths to monitor during chromatographic experiments. Samples were placed in a quartz cuvette and spectra were collected over the a range from 200 – 800 nm. Instrument resolution was 1.5 nm.

4.3.1.2 Raman Spectroscopy

The bulk of the Raman spectra recorded in this work used a DeltaNu Advantage 785 Raman spectrometer (SciAps, Woburn, MA). This spectrometer is fitted with a 785 nm diode laser, an air cooled CCD detector, and has a resolution of 4.0 cm^{-1}. The spectrometer was operated with NuSpec software for signal acquisition and processing.

EC-SERS work was done using a DXR Smart Raman Spectrometer (Thermo Fisher Scientific, Mississauga, ON, Canada). This spectrometer has the ability to use two different laser excitation wavelengths: 532 nm and 780 nm, and can be fitted with two different gratings: a full range, low resolution (5 cm^{-1}) grating, and a shorter range, high resolution (3 cm^{-1}) grating. This thesis work used only the 780 nm laser line with the high resolution grating, as using a lower energy wavelength results in lower background fluorescence. This Raman spectrometer was used for the EC-SERS work since it is also coupled to a potentiostat, which is necessary for electrochemical measurements.

An acquisition time of 30 s and a laser power setting ranging between 12 and 27 mW was used for collecting Raman spectra with both the 785 nm and 780 nm laser lines. For all further spectral processing and data analysis was completed using Origin 9.0 (OriginLab Corporation, Northampton, MA) on a standard PC. All data measured were corrected for acquisition time and laser power, and also smoothed using a 9 point adjacent/averaging smoothing method.

4.3.2 Electrochemistry

A Pine Research Instrumentation portable USB Wavenow potentiostat/galvanostat (Durham, NC, U.S.A.) was used for conducting electrochemical measurements with the electrochemical software, Aftermath Data Organizer (version 1.2.4361), also produced by Pine Research Instrumentation.

4.3.2.1 Electrochemical Surface-Enhanced Raman Spectroscopy (EC-SERS)

Screen printed electrodes (SPE) (15 x 61 x 0.36 mm) were purchased from Pine Research Instrumentation (Durham, NC, U.S.A.). They consist of a silver/silver chloride (Ag/AgCl) reference electrode, a carbon counter electrode, and a 5 x 4 mm carbon working electrode. The working electrode was then modified with Ag nanoparticles and surface treatments as outlined in section 4.4.3 rendering the electrode SERS active. Modified SPEs were placed in the electrochemical cell, which was a standard glass vial. 0.1 M NaF was used as the supporting electrolyte and was purged with argon (99.999%, Praxair Canada Inc., Ontario, Canada) prior to use, and was added to the electrochemical cell containing the SPE. The open circuit potential (OCP) spectrum could then be collected. This spectrum is an important reference as it represents the SERS signal achievable at the resting potential of the metal (i.e. SERS without any electrochemical contribution). The system was first stepped in the cathodic direction (0.0 V to -1.0 V) and then the anodic direction (-1.0 V to 0.0V), both in increments of 0.1V. At each applied potential a SERS spectrum was collected. All potentials are reported versus Ag/AgCl reference electrode.

4.3.3 Scanning Electron Microscopy

Scanning electron microscopy (SEM) images were acquired using Tescan MIRA3 LMU Field Emission SEM (Warrendale, PA, U.S.A.). This FE-SEM has a tungsten electron gun and is fitted with both a back scatter and a secondary electron detector.

4.3.4 Liquid Chromatography

4.3.4.1 One-Dimensional Liquid Chromatography

Single dimension liquid chromatographic analysis was carried out on an Agilent 1290 Infinty II series UHPLC system (Agilent Technologies, Santa Clara, CA). Mobile

phases of (A) 0.1% formic acid in water and (B) 0.1% formic acid in methanol were used. After optimization, the gradient elution used was as follows: 0 min at 50%B, 3 min at 55%B, 10 min at 80%B, and 11 min at 95%B. An Agilent ZORBAX SB-C18 (2.1 × 100 mm × 1.8 µm) column was maintained at 30 °C throughout the entire run (stop time = 15 min). An extract volume of 1.5 µL was injected into the system using an auto-sampler and a flow rate of 0.2 mL / min was used. UV-vis spectra were collected at 350 nm for pure samples and 327 nm for mixtures using a diode array detector (DAD), with a reference wavelength of 500 nm and a bandwidth of 50 nm.

Samples were prepared in a MeOH / H_2O solution and filtered with 0.2 µm polytetrafluoroethylene (PTFE) syringe filters.

4.3.4.2 Two-Dimensional Liquid Chromatography

Multidimensional liquid chromatographic analysis was carried out on the same system. The first dimension separation was exactly as outlined above. The second dimension used mobile phases of (A) 0.1% formic acid in water and (B) 0.1% formic acid in acetonitrile, formic acid obtained from Anachemica (Montreal, QC) and acetonitrile obtained from Sigma Aldrich (St. Louis, MO). The second dimension uses a two minute run time with a gradient as follows: 0 min at 5%B and 1.4 min at 95%B. An Agilent ZORBAX BONUS RP (2.1 × 50 mm × 1.8 µm) column was used with a maintained temperature of 30 °C. An extract volume of 2.0 µL was injected using an auto-sampler and a flow rate of 1 mL / min was used in the second dimension while 0.2 mL / min was used in the first dimension. A threshold of 20 mAU was used to trigger heart-cutting from the first dimension to the second dimension and a threshold of 2.5 mAU to trigger fraction collection into an Agilent 96-well plate. UV-vis spectra were again collected at

327 nm, with a reference wavelength at 500 nm and a bandwidth of 50 nm using a diode array detector.

2D-LC-SERS analysis was completed by drop coating the collected fraction onto pre-treated filter paper SERS substrates in 5 µL aliquots, which were allowed to briefly air dry, and were then analysed using SERS.

4.4 Surface-Enhanced Raman Spectroscopy Substrates

4.4.1 Silver Nanoparticle Synthesis

The following method for silver nanoparticle preparation is adapted from Zhao *et al.*[76] 95.0 mL of Millipore water, 1.0 mL of 0.1M $AgNO_3$, 3.4 mL of 5% w/w sodium citrate, and 0.6 mL of 0.17 M citric acid were all added to a three necked, flat bottom flask and stirred. A 200 µL aliquot of a 0.1 mM solution of $NaBH_4$ was then added to the mixture and left to react for one minute. The mixture was then allowed to boil under reflux for 80 minutes before being cooled to room temperature. The colloidal Ag was portioned into 14 centrifuge tubes, each containing 1.43 mL and centrifuged for 20 min at 8000 rpm. The resulting supernatant was removed and the remaining Ag "paste" was combined into one tube and the centrifugation step repeated. The supernatant was removed again and the final amount of AgNP paste was made up to 50 µL using millipore water.

4.4.2 Three-Dimensional Surface-Enhanced Raman Spectroscopy Substrate Preparation

The 3D SERS substrates were created using 47 mm glass fiber filters (Gelman, Ann Arbour, MI, USA), 0.45 µm nitrocellulose membrane filters (Whatman, Maidstone, UK), 37% silk, 35% hemp, 28% cotton blend fabric (Pickering International, Inc. San Francisco, USA), Ahlstrom grade 631 cellulose based filter paper (Whatman, Maidstone,

UK), and 0.02 µm porous alumina (Whatman, Maidstone, UK). The 3D materials were cut into approximately 5 x 4 mm rectangles and AgNP paste was drop coated onto the FP in 3 layers of 5µL; each layer was allowed to dry fully prior to the application of another layer. After the final layer was dried, a 5 µL sample of analyte (1 mM) was drop coated onto the substrate and analysed. Analysis included SEM characterization, SERS characterization of spot-to-spot signal variation, and comparison of signal intensity to one another.

The filter paper (FP) substrates outperformed the other materials and thus three different laboratory filter papers (Ahlstrom grade 631, Fisher grade P5, and Whatman grade 1) were chosen and compared (Table 4.1).

Table 4.1: Comparison of properties for different filter paper brands.

	Ahlstrom (Grade 631)	**Fisher (Grade P5)**	**Whatman (Grade 1)**
Thickness (mm)	0.23	0.17	0.18
Particle Retention (µm)	25	10	11
Flow Rate (mL/min)	200	60	55
Loading Capacity	High	Medium	Medium

4.4.3 Substrate Surface Modifications

Both a displacement of capping agents and functionalization of the nanoparticle surface needs to be carried out in order to detect the phenolic compounds. The capping agents that are used to stabilize and protect NPs can become problematic when doing

SERS measurements as their signals can overshadow that of the analyte. In this work, the FP substrates were allowed to incubate in a 0.5 M solution of KCl for 30 minutes, after which they were rinsed with Millipore water and allowed to air dry. Due to the strong specific adsorption of Cl^- onto the Ag surface, it is able to displace capping agents, allowing the analyte to be detected once sequentially introduced.[77,78]

Due to the poor adsorption of phenolic compounds onto the AgNP surface, a functionalization of the surface needs to be performed in order to more closely attract these molecules to the surface, thereby aiding in their detection by SERS. Pyridine was chosen as a candidate for surface functionalizing based on a study by De Bleye et al.[79]. This study showed evidence that by modifying a Ag nanoparticle surface with pyridine it improved the SERS signal for the detection of bisphenols. In this approach, the KCl-treated FP substrates were further incubated in a 1 mM aqueous pyridine solution for one hour before being rinsed with Millipore water and air dried. SERS performance was then evaluated using four polyphenol standards.

4.5 Electrochemical-Surface-Enhanced Raman Spectroscopy Substrate Preparation

For electrochemical SERS (EC-SERS) investigations carbon screen printed electrodes (SPEs) were prepared using similar methods to pervious work.[77,78] AgNP paste was drop coated onto the rectangular 4 x 5 mm working electrode in 3 layers of 5µL; each layer was allowed to dry fully prior to the application of another layer. After the final layer was dried, SPEs were allowed to incubate in a 0.5 M solution of KCl for 30 minutes, after which they were rinsed with Millipore water and allowed to air dry. Finally, a 5 µL sample of pyridine (100 mM) was drop coated onto the substrate and analysed. The SPE features a built-in counter electrode (carbon) and reference electrode (Ag/AgCl). All electrolyte solutions were purged with argon gas prior to measurement.

Chapter 5: Results and Discussion

5.1 Comparison of Three-Dimensional (3D) Surface-Enhanced Raman Spectroscopy Substrates

A three-dimensional (3D) SERS substrate was chosen due to the increased surface area and the higher chance of interaction with analytes compared to 2D substrates. Five three-dimensional materials [blend fabric (37% silk, 35% hemp, 28% cotton), glass fiber filter, nitrocellulose membrane filter, cellulose based qualitative filter paper, and porous alumina] were selected and tested to observe which gave a more intense SERS signal for the standard test flavonoid molecule, luteolin. In Figure 5.1, scanning electron microscopy (SEM) images of each substrate can be seen and Figure 5.2 shows the SERS spectra for each substrate with identical treatments of 0.5 M KCl and 1.0 mM pyridine and addition of 5 µL of 1.0 mM luteolin. It can be seen that the standard laboratory filter paper (FP) out performed all other materials by a significant margin and hence all further studies focused on filter paper based substrates.

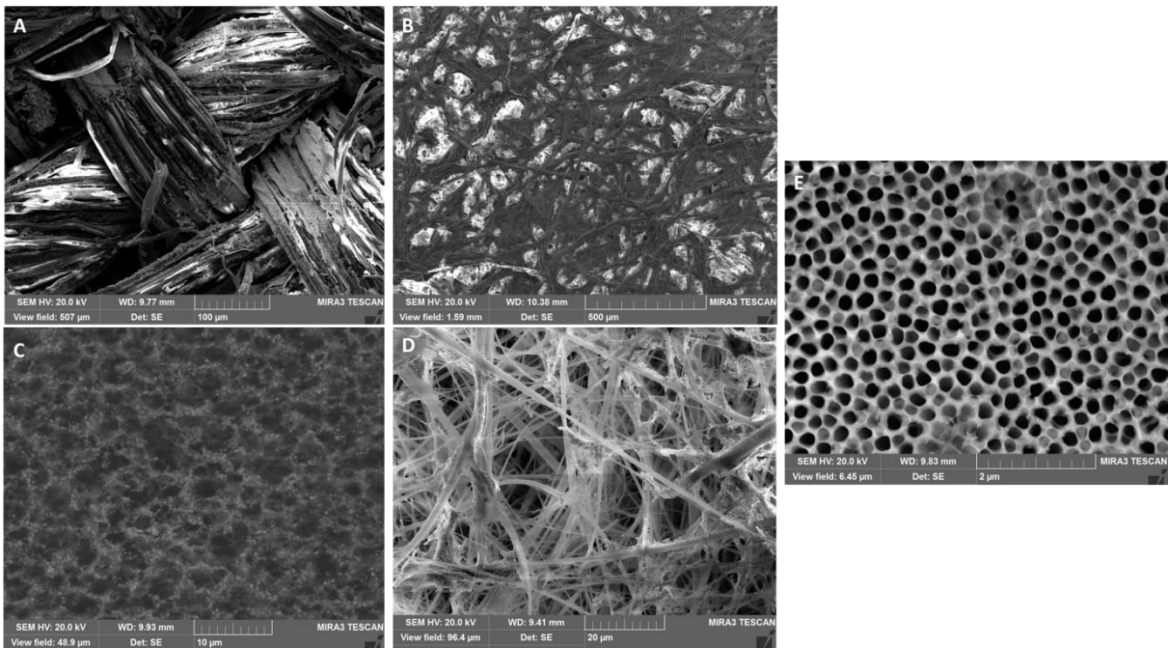

Figure 5.1: (A) Blend fabric, (B) filter paper, (C) nitrocellulose membrane, and (D) glass fiber filter SEM images with silver nanoparticles. (E) Porous alumina SEM image is shown without nanoparticles for ease of viewing the 3D structure.

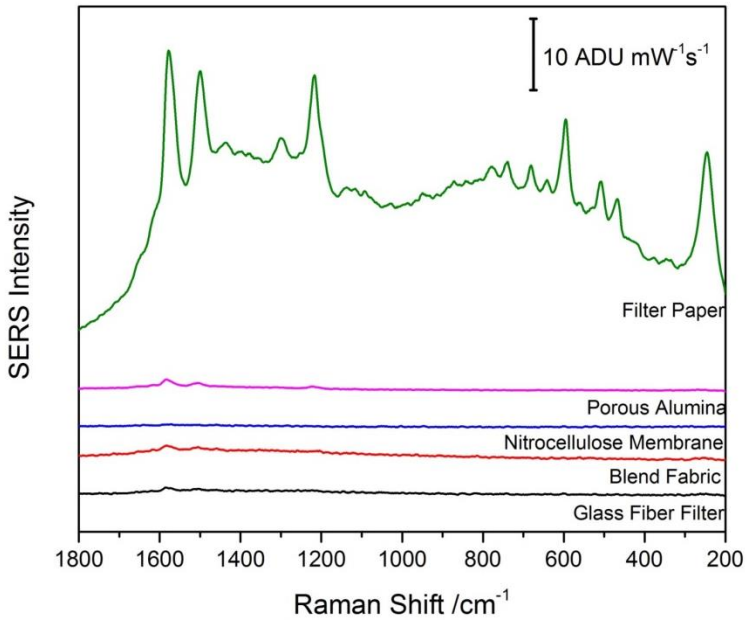

Figure 5.2: Comparison of SERS spectra of different substrates with 1.0 mM luteolin (30 s, 12.17 mW, 785 nm laser).

Since the filter paper far out performed the other substrates in terms of the resulting SERS signal intensities, a subsequent investigation of different filter papers by different manufacturers was undertaken and their resultant SERS signals were compared. It can be seen in Figure 5.3 that Ahlstrom filter paper, grade 631, gave the spectrum with the greatest SERS intensity when signals were compared for 1.0 mM luteolin. A possible explanation as to why this brand outperformed the others is because the Ahlstrom paper (grade 631) has a high loading capacity, whereas the Fisher (Qualitative P5) and Whatman (Grade 1) papers have medium loading capacities (Table 4.1).[80] This would allow more nanoparticles to be present on the substrate and thus create more opportunity for SERS enhancement. SEM images of the different brands of filter paper after the addition of nanoparticles are shown in Figure 5.4. All images show comparable amounts of nanoparticles on the surface. However, the Ahlstrom FP shows more white areas in the images due to the charging effect. This suggests that the density of the nanoparticles on this substrate is larger, thus explaining why there is an increase in SERS signal intensity.

Therefore, moving forward in this research Ahlstrom filter paper (grade 631) was used for the preparation of all FP SERS substrates.

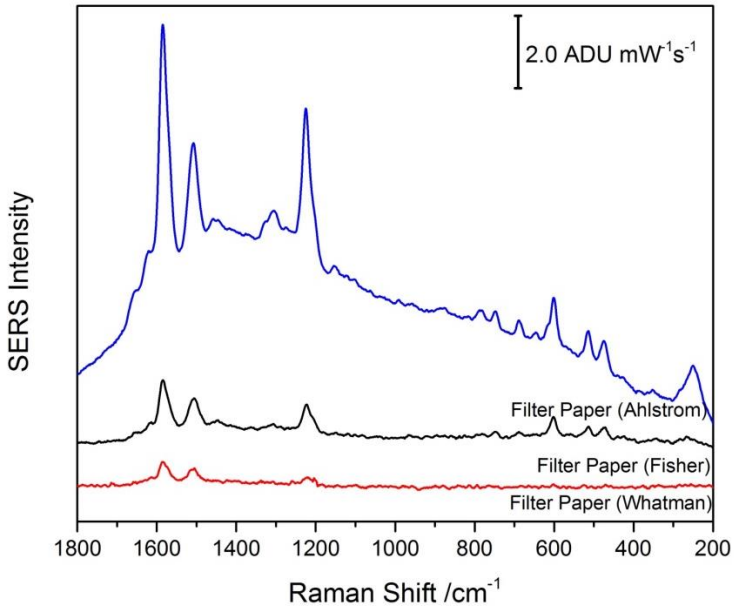

Figure 5.3: Comparison of SERS spectra for 1.0mM luteolin of different filter papers (Ahlstrom, Grade 631; Fisher, Qualitative P5; Whatman, Grade 1) (30 s, 12.17 mW, 785 nm laser).

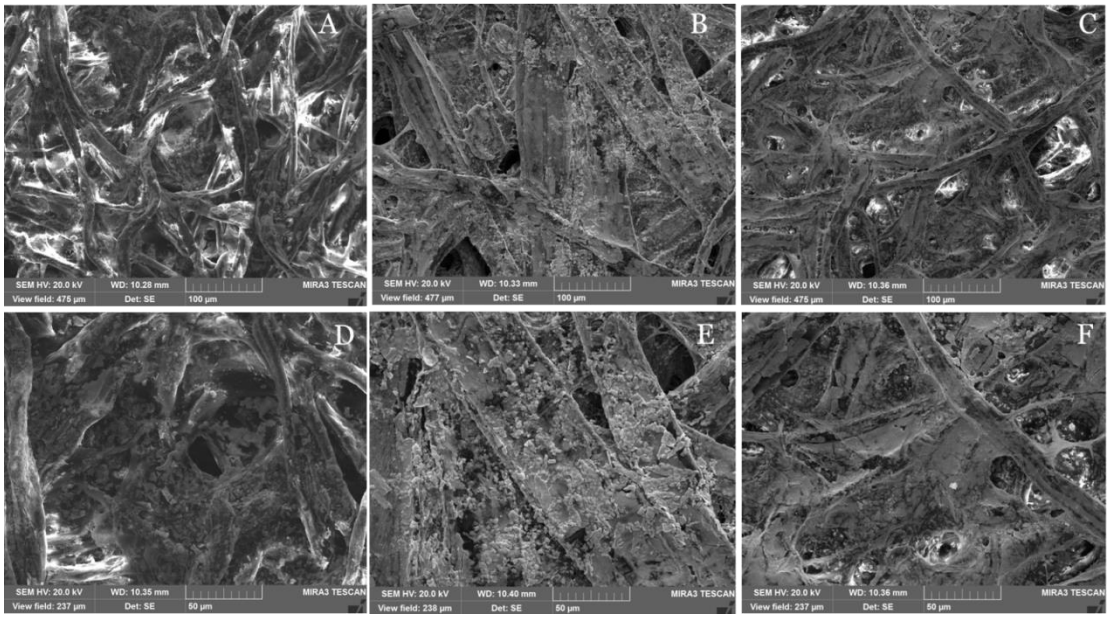

Figure 5.4: SEM images of Ahlstrom (A&D), Fisher (B&E), and Whatman (C&F) filter paper substrates with Ag nanoparticles. A-C shows images at 500x magnification, and D-F shows images at 1000x magnification.

5.2 Pyridine Functionalization of 3D Surface-Enhanced Raman Spectroscopy Substrates

As shown by previous research in our group[77,78], it was noted that a citrate displacement treatment was essential to receiving clear and enhanced SERS signal. This is due to the use of citrate as the reducing agent in the nanoparticle synthesis. Citrate ion is a large negatively charged species that is attracted to the nanoparticle surface. The signal from citrate can often obscure the signal for the desired analyte or can physically block the analyte from reaching the surface and benefiting from the SERS enhancement. Thus, a solution of potassium chloride (KCl) is used to displace the citrate from the metal surface and replace it with a much smaller ion, Cl^-.[77,78] This displacement occurs due to the strong specific adsorption of chlorine onto silver surfaces. This treatment is necessary for the filter paper substrates as well. By incubating the FP substrates in a 0.5 M potassium chloride (KCl) solution for 30 minutes, the chloride ions displaced the large, negatively charged citrate molecules. However, even with citrate displacement the signal for the flavonoid and phenolic acid analytes was not able to be seen; therefore additional functionalization strategies were explored. In 2015, De Bleye et al. were able to detect bisphenols by functionalizing their SERS substrates with pyridine (pyr).[79] This functionalization technique was shown to greatly aid in the detection of flavonoids and phenolic acids in the present thesis work (Figure 5.5). An analogous functionalization strategy explored the use of pyrazine (pyz), which has a similar structure to pyr (Figure 5.6), but with the additional nitrogen atom (and thus another lone pair susceptible to bonding) was also investigated (Figure A.2). Functionalization with pyz resulted in lower intensity in analyte signal, and pyridine functionalization was therefore chosen to be the optimal strategy for detection of polyphenolic compounds.

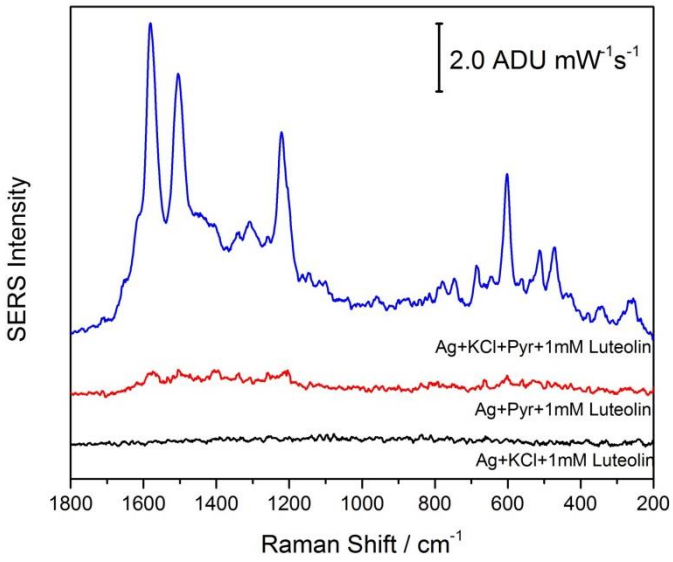

Figure 5.5: SERS signal of 1mM luteolin on filter paper substrates with different optimization strategies. Show with solely KCl treatment (black), with solely pyridine functionalization (red), and with KCl treatment followed by pyridine functionalization (blue) (30 s, 12.17 mW, 785 nm laser).

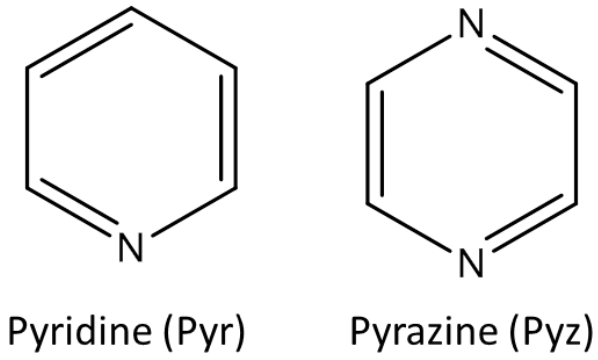

Figure 5.6: Structures of pyridine (pyr) and pyrazine (pyz).

Although this pyridine functionalization strategy worked especially well for this application, in the paper by De Bleye et al. (and in subsequent work by others[81]) the role pyridine plays in the improvement of the SERS signal was not well explained.[79,81] De Bleye et al. explained that pyridine is known to strongly interact with metals through the formation of a covalent bond through the lone pair of electrons present on the nitrogen

atom. Despite this well-known interaction, they claim that the enhancement is also due to the nitrogen of pyridine. This time forming hydrogen bonds with the hydroxyl functionalities of the analyte, these two thoughts are seemingly contradictory. Since it was clear in the present work that a pyridine functionalization strategy was needed for efficient SERS detection of polyphenols, this current thesis work took a slight diversion in order to elucidate the reason behind this improved signal.

Pyridine has been used historically in both Raman spectroscopy and SERS and has a very strong Raman signal.[48,82,83] However, in the present work no substantial signal for pyridine was observed, even when it was supposedly the only substance present on the surface. To better understand what could be happening on the surface, electrochemical surface-enhanced Raman spectroscopy (EC-SERS) studies were conducted for the modified screen printed electrodes (treated with both KCl and 100 mM pyr). 100 mM aqueous pyridine solution was used as the analyte; an increased concentration of the pyr compared to the treatment of the FP substrates was used to more clearly see the potential-dependant changes in signal. The electrode was placed into an electrochemical cell with a supporting electrolyte of 0.1 M aqueous sodium fluoride (NaF). Voltage was then applied to the surface and subsequent SERS measurements were taken at each voltage. Voltages progressed in the cathodic direction from 0 V to -1.0 V in a 100 mV step wise fashion, and in the anodic direction from -1.0 V to 0 V in a 100 mV step-wise fashion.

The metal-surface selection rules predict that bands that correspond to molecular vibrations with an oscillating polarizability tensor parallel to the surface will be supressed, while molecular vibrations with an oscillating polarizability tensor perpendicular to the surface are enhanced .[84,85] Thus in this experiment, signals for ring breathing of pyr will be suppressed when the molecule is planar to the surface and will be

observed when the molecule is perpendicular to the surface. Figure 5.7 shows the results from this experimentation in which the signal for perpendicularly bound pyridine, [1,006 cm^{-1}(total symmetric ring breathing), 1,027 cm^{-1} (trigonal ring breathing)][86] appears only when a negative potential is applied to the surface. It is theorized that pyridine must reorient on the surface once there is a potential applied and that at open circuit potential (OCP) (in the absence of applied potential - the potential which the filter paper substrates of this study are normally subjected to) pyridine is adsorbed on the surface of the nanoparticles in a planar orientation (Figure 5.8). This opens up both the lone pair of electrons on the nitrogen atom and the double bond nature of the pyridine ring to both be able to interact with the analyte molecules and draw them closer to the surface, thus aiding in the SERS analysis. Hence, this EC-SERS study suggests that the most likely nature of the interaction between the luteolin and the pyridine molecules is via strong van der Waals intermolecular interactions.

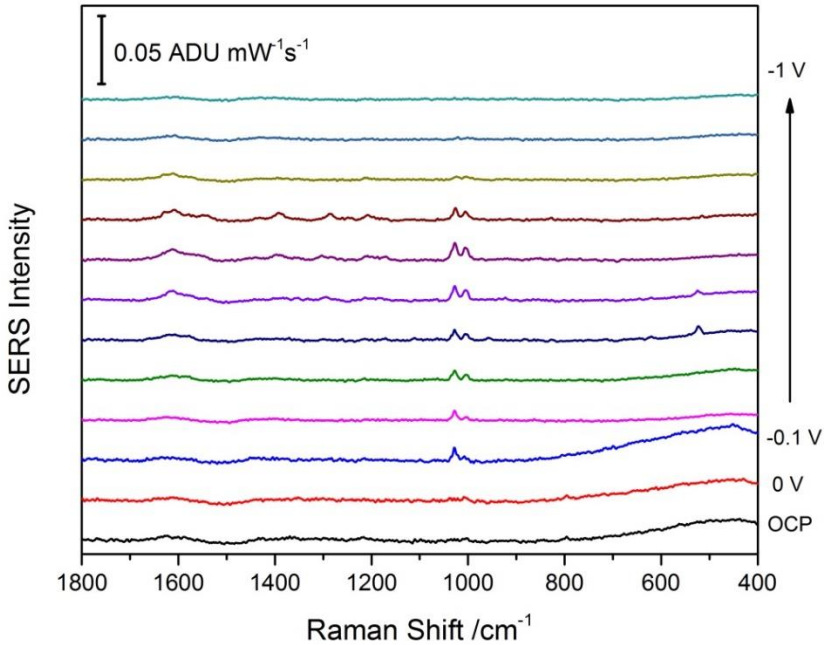

Figure 5.7: EC-SERS analysis of 100 mM pyridine on the surface of AgNP coated screen printed electrode. (Cathodic, 0.1V step-wise progression from 0V to -1V) (30 s, 80 mW, 780 nm laser).

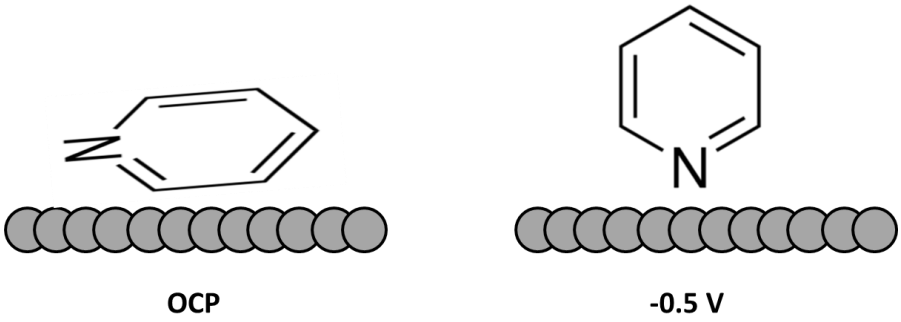

Figure 5.8: Scheme for the orientation of pyridine on a silver nanoparticle surface at open circuit potential (OCP) and -0.5 V.

5.3 Filter Paper Surface-Enhanced Raman Spectroscopy Substrate Analysis of Polyphenols

The FP SERS substrates were used for the detection of four different analytical polyphenol standards: quercetin, luteolin, chlorogenic acid, and caffeic acid (Figure 5.9). These standards were chosen as they are some of the most prevalent polyphenols and SERS signal for each have been previously reported.[87–90] Raman spectra (Figure 5.10) of the pure powder for each sample were collected in order to confirm the compound identity via SERS. The Raman spectra represent the various vibrational modes present in the molecule, which collectively make up a vibrational "fingerprint" of each molecule.

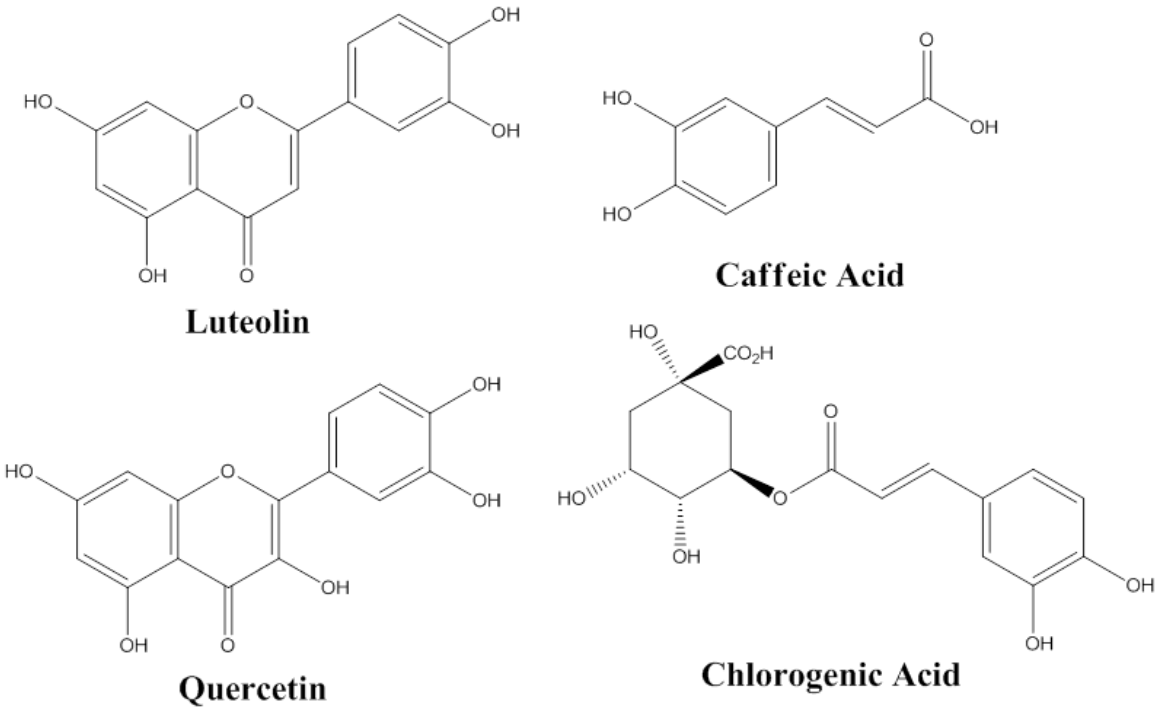

Figure 5.9: Structures of luteolin, caffeic acid, quercetin, and chlorogenic acid.

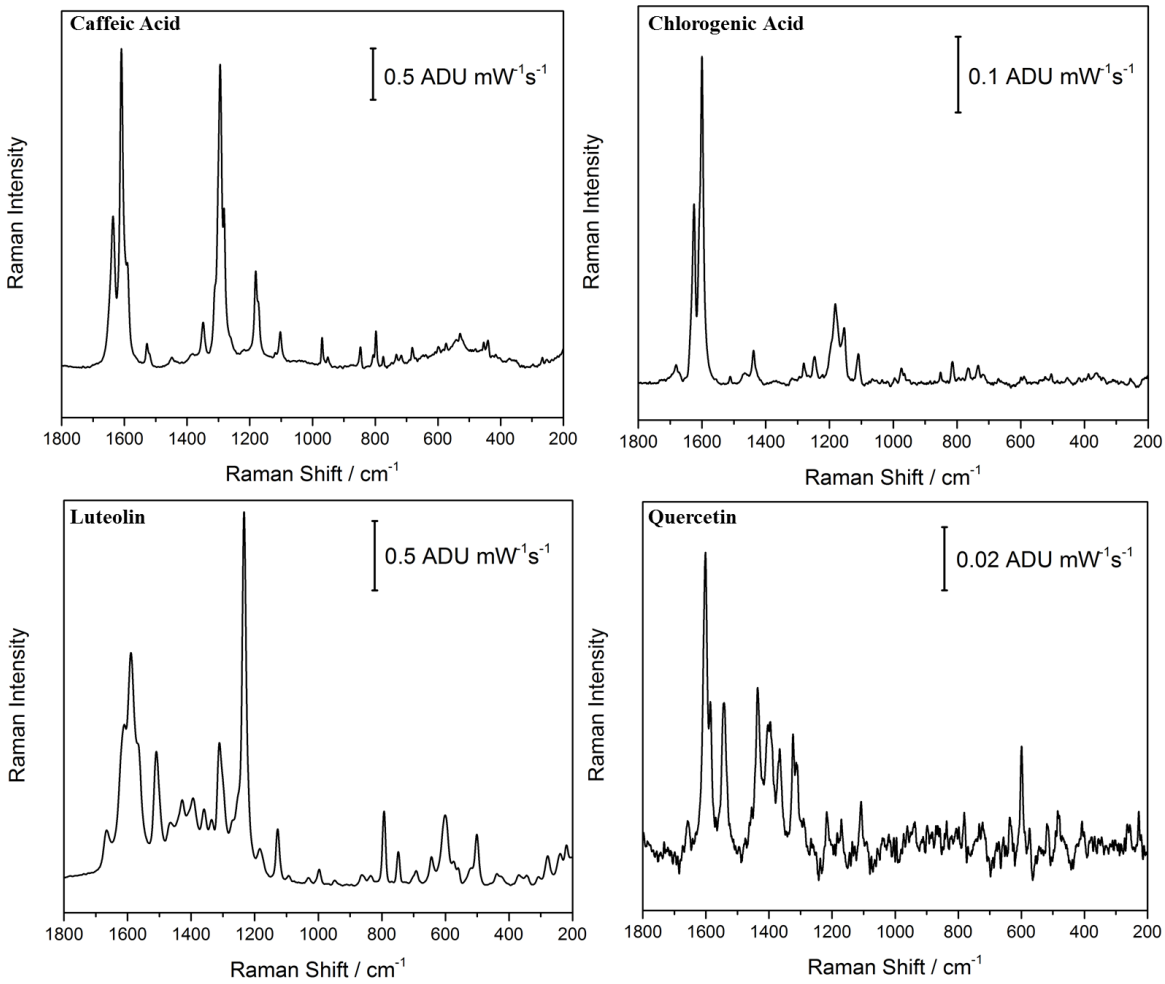

Figure 5.10: Raman spectra of caffeic acid, chlorogenic acid, luteolin, and quercetin (30 s, 80 mW, 780 nm laser).

Analytes were drop coated onto the FP substrates after KCl and pyridine treatments and subsequently analysed using SERS. SERS signal could be obtained for 1.0 mM concentrations of the four analytes as seen in Figure 5.11. When thinking forward to the ultimate goal of this research, which is to collect SERS signal from the end of a 2D-LC run, 50 ppm of analyte would be a more comparable and relevant concentration to analyze. Thus, the SERS signal for 50 ppm of each analyte can be seen in Figure 5.12. Once all four standards could be detected at 50 ppm using the modified FP substrates, the thesis research moved onto the 2D-LC separation work.

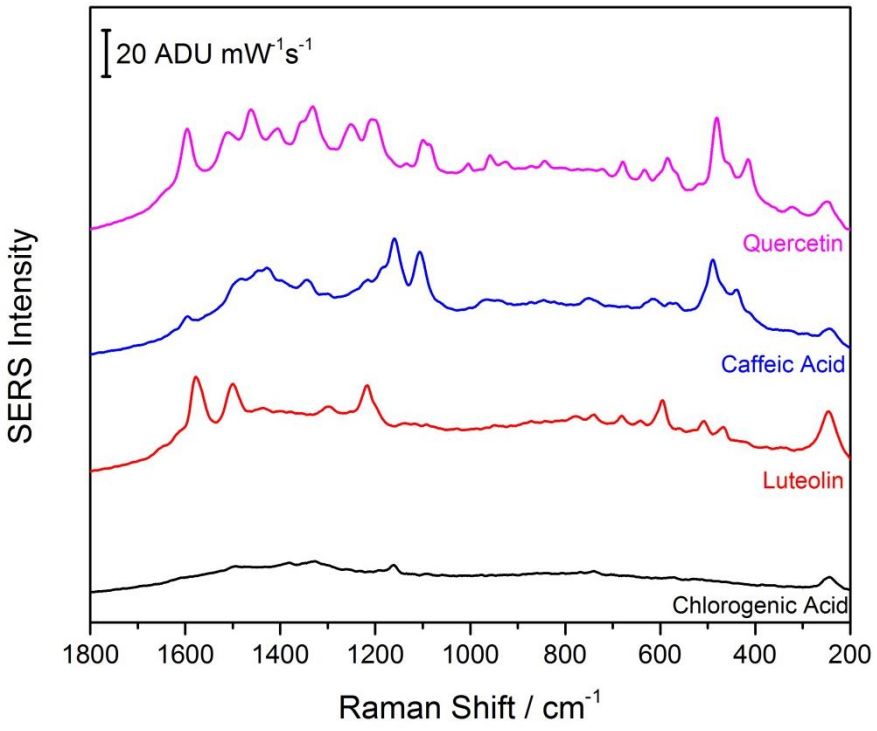

Figure 5.11: SERS signal of 5 µL of 1.0 mM of each analyte: luteolin (286 ppm), chlorogenic acid (354 ppm), caffeic acid (180 ppm), and quercetin (203 ppm) (30 s, 12.17 mW, 785 nm laser).

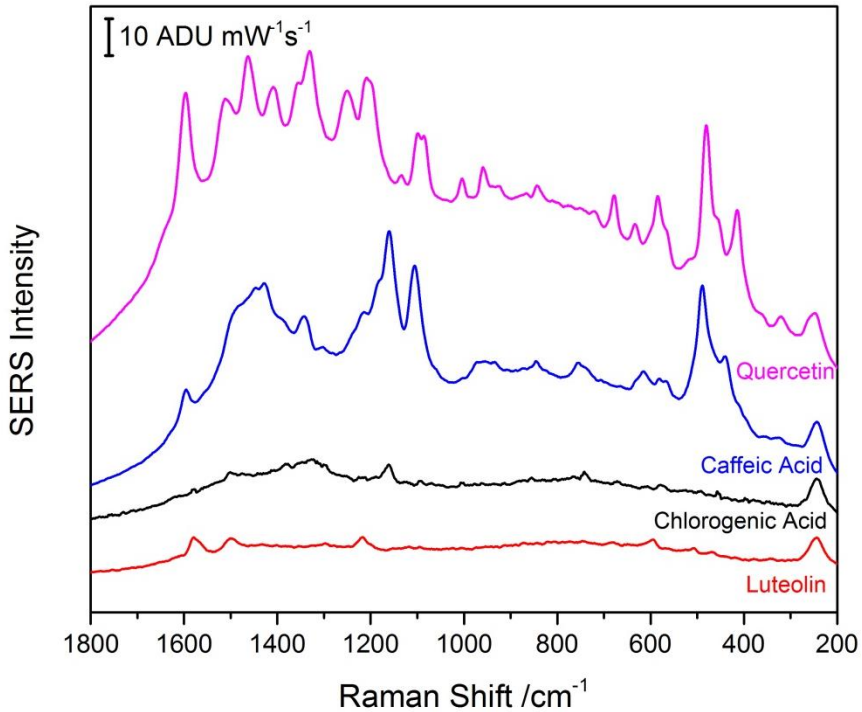

Figure 5.12: SERS signal of 5 µL of 50 ppm (of each analyte: luteolin, chlorogenic acid, caffeic acid, and quercetin) (30 s, 12.17 mW, 785 nm laser).

5.4 Multidimensional Liquid Chromatographic Separations of Polyphenols

5.4.1 Characterization of Standards

In order to characterize each standard, 100 ppm solutions (20:80, MeOH:H_2O) were analysed using 1D liquid chromatography; 10 µL aliquots are injected into the instrument and separated using gradient elution. To know which wavelength the chromatograms should be monitored at the diode array detection (DAD), the UV-vis spectrum of a 25 ppm mixture of the standards was recorded (Figure 5.13). This spectrum shows a large absorbance at 327 nm, therefore DAD detection is taken around this wavelength (350 nm for the separate standards and 327 nm for the mixtures in section 5.4.2). The chromatograms for each analytical standard are shown in Figure 5.14 with the retention times being 4.76, 5.71, 10.21, and 10.74 minutes for chlorogenic acid, caffeic acid, quercetin, and luteolin respectively.

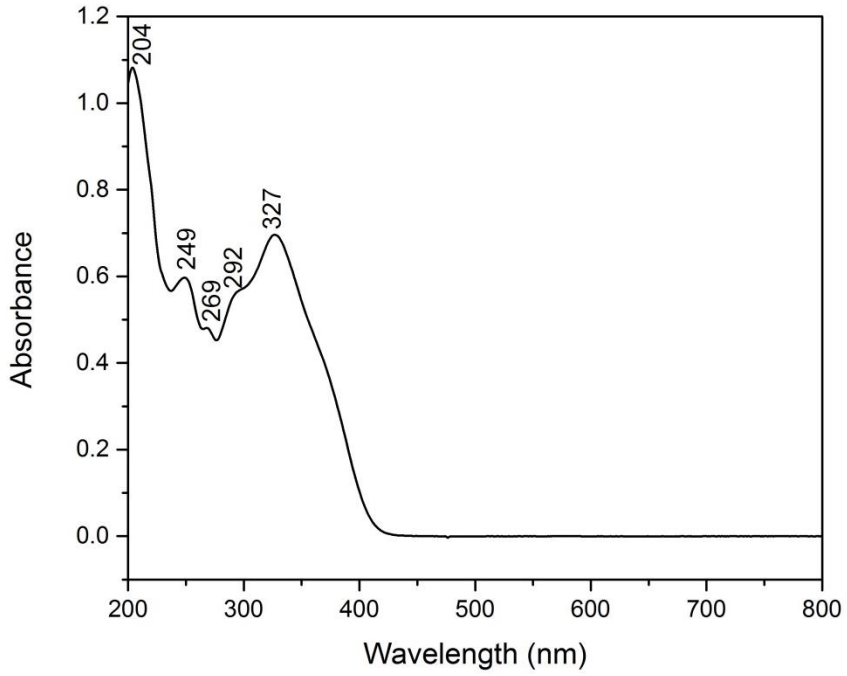

Figure 5.13: UV-vis absorbance spectra of a 25 ppm mixture of luteolin, quercetin, chlorogenic acid, and caffeic acid, diluted 1:10 with MeOH:H_2O (50:50 % v/v).

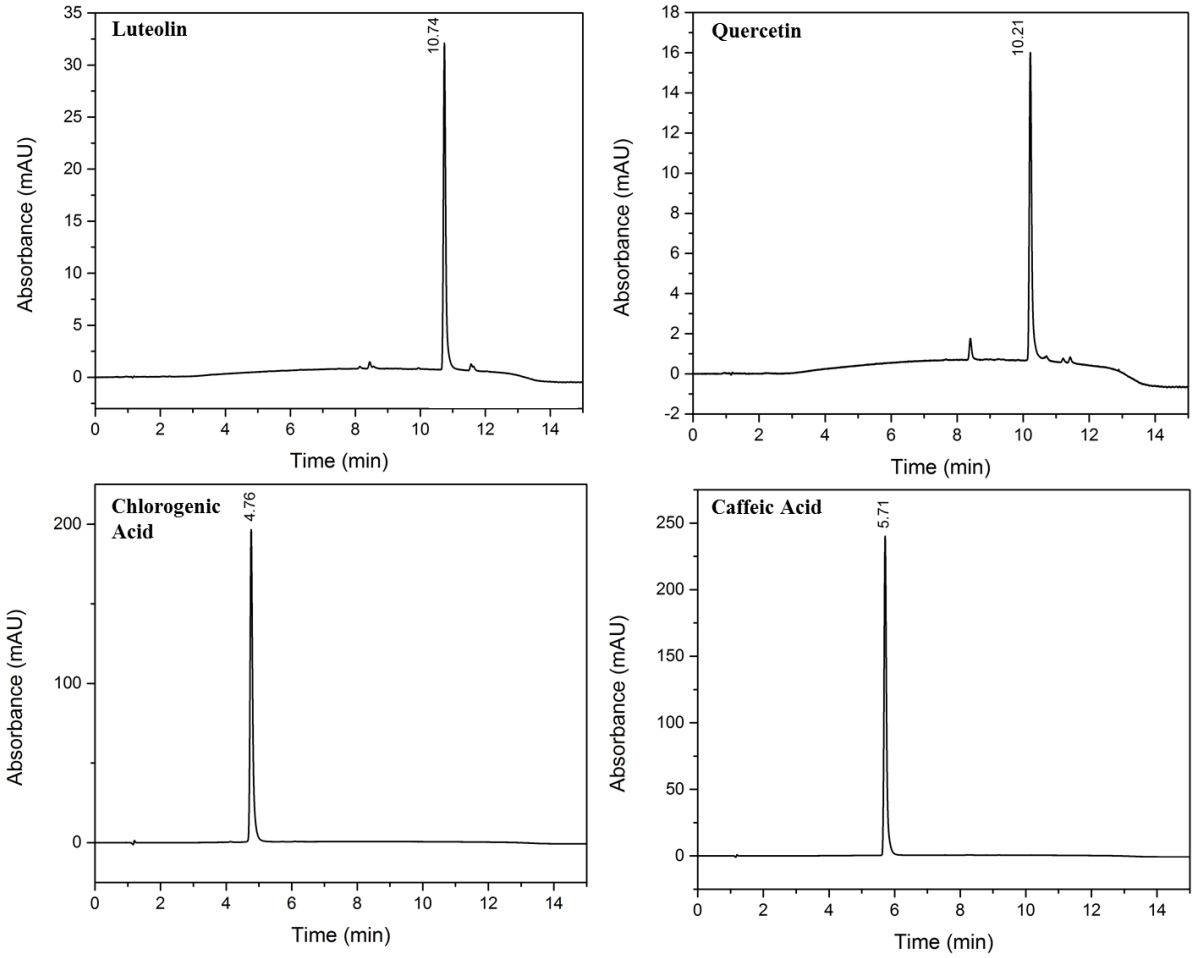

Figure 5.14: ^{1}D chromatograms for 100 ppm (20:80% v/v, MeOH:H_2O) solutions of luteolin, quercetin, chlorogenic acid, and caffeic acid at 350 nm with retention times stated above each main peak.

5.4.2 Separation of Mixture

In order to ensure each standard could be separated out from a mixture, a 25 ppm mixture in MeOH:H_2O (20:80% v/v) was prepared by combining the 100 ppm solutions of each standard to the sample vial (a final concentration of 25 ppm for each species) and the mixture was subsequently analysed using 1D-LC. A 1.0 µL aliquot was injected onto the instrument and analysed using the same parameters as each separate standard. The ^{1}D chromatogram of the separated mixture can be seen in Figure 5.15 where the retention times parallel those of the pure standard. The retention times of 4.76, 5.70, 10.22, and

10.70 min relate to chlorogenic acid, caffeic acid, quercetin, and luteolin respectively. The latter two peaks are much lower in intensity, and this was attributed to solubility issues in 20% MeOH for these species.

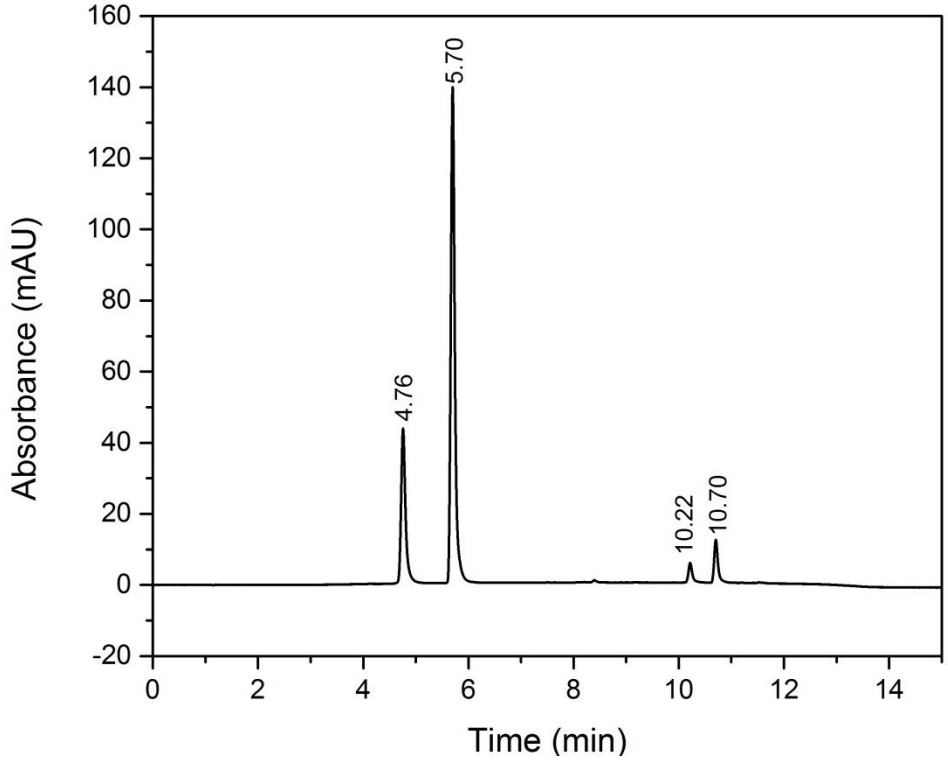

Figure 5.15: [1]D chromatogram for the 25 ppm (20:80% v/v, MeOH:H_2O) mixture of luteolin, quercetin, chlorogenic acid, and caffeic acid at 350 nm with retention times stated above each main peak.

To overcome the solubility issues observed in the 1D separation, the 25 ppm mixture was prepared using MeOH:H_2O (50:50% v/v) and to combat any potential solubility issues within the instrumentation, the gradient elution was initiated at this same composition. The methodology is outlined in Table 5.1. Starting at a solvent composition with a higher percentage of organic solvent allowed for faster elution of analytes, thus the retention times were shorter, but the order in which the standards elute remained the same (Table 5.2, Figure A.1). [1]D separation of the four analytes under these new conditions gave retention times of chlorogenic acid (1.26 min), caffeic acid (1.59 min), quercetin

(5.07 min), and luteolin (6.15 min). This can be seen in Figure 5.16, the ^{1}D chromatogram in which the retention times are reduced by half, but the relative elution order was maintained. The dotted line reflects the threshold at which peaks were selected to be sampled and transferred to the second dimension. In this case a threshold of 20 mAU was chosen, and any analyte with absorbance detected at or above this limit was placed in a sample loop to be separated in the second dimension.

Table 5.1: 1D-LC methodologies for the separation of polyphenolic compounds.

	Initial Method	**Optimised Method**
First Dimension Column	Agilent ZORBAX SB-C18 (2.1 x 100 mm x 1.8 µm)	Agilent ZORBAX SB-C18 (2.1 x 100 mm x 1.8 µm)
Sample	20:80% v/v MeOH:H_2O	50:50% v/v MeOH:H_2O
Solvent A	0.1% Formic Acid in Water	0.1% Formic Acid in Water
Solvent B	0.1% Formic Acid in Methanol	0.1% Formic Acid in Methanol
Flow Rate	0.2 mL / min	0.2 mL / min
Gradient	20 %B at 0 min 80 %B at 10 min 95 %B at 11 min	50 %B at 0 min 55 %B at 3 min 80 %B at 10 min 95 %B at 11 min
Column Temperature	30 °C	30 °C

Table 5.2: Comparison of retention times for analytical standards with differing sample diluent composition, 20:80 % v/v and 50:50 % v/v MeOH and H_2O, and gradient elution methodology.

Standard	**1D -Retention Time Initial Method**	**1D -Retention Time Optimised Method**
Chlorogenic Acid	4.76 min	1.28 min
Caffeic Acid	5.71 min	1.61 min
Quercetin	10.21 min	5.06 min
Luteolin	10.74 min	6.14 min

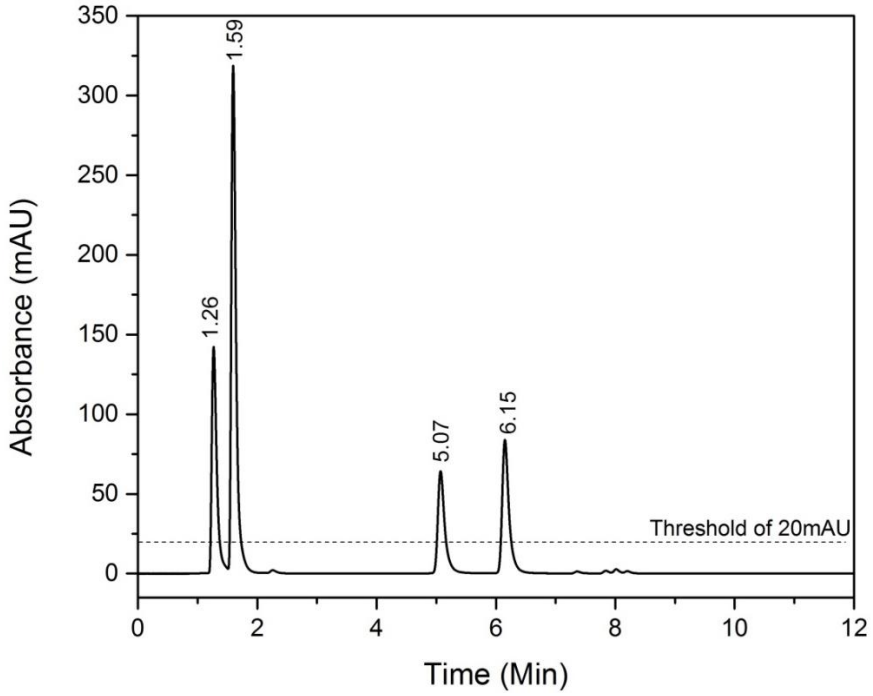

Figure 5.16: [1]D chromatogram of 25 ppm mixture (50:50% v/v, MeOH:H_2O) at 327 nm with a [2]D threshold of 20 mAU.

The second dimension chromatogram can be seen in Figure 5.17, where the peaks denoted with an asterisk correspond to the analytes selected from the first dimension. As these analytes were pure analytical standards, as suspected there was only one analyte present for each second dimension separation. As the second dimension does not

necessarily analyse peaks in the order that they are collected, the analytes denoted in Figure 5.17 are not in the same order as previously stated in the first dimension separations. The peaks marked from earliest eluted to latest correlate to chlorogenic acid, caffeic acid, luteolin, and quercetin respectively. The dotted line reflects the threshold set for fraction collection. In this case, any analyte that absorbs higher than 2.5 mAU will be collected into a sampling tray (96-well plate) and used for further investigation, which in relation to this thesis work will be SERS analysis using the optimized FP substrates.

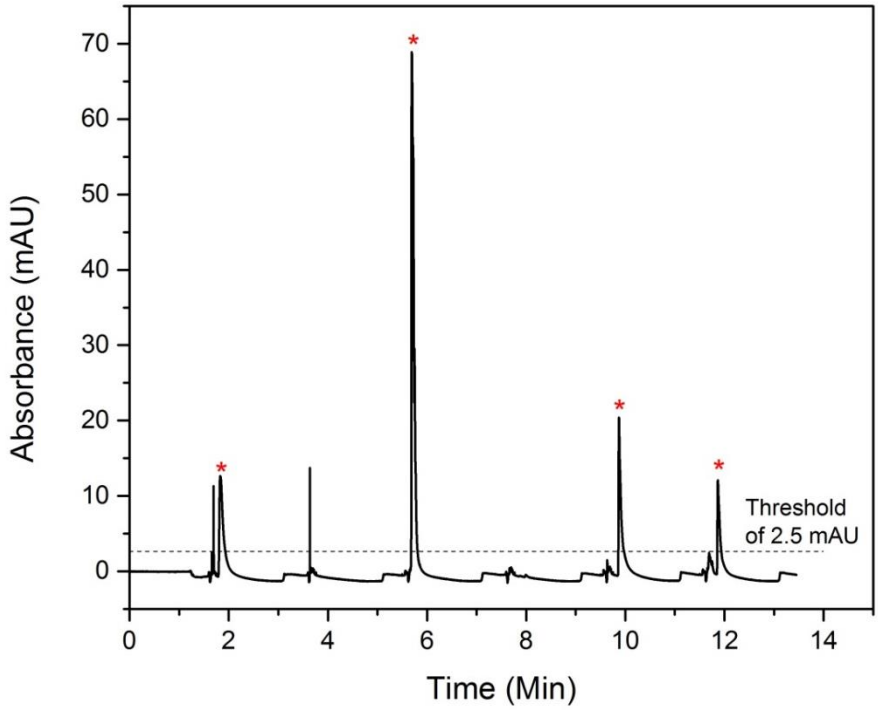

Figure 5.17: ^{2}D chromatogram of 25 ppm mixture (50:50% v/v, MeOH:H_2O) at 327 nm with a fraction collection threshold of 2.5 mAU. Peaks with asterisks correspond to the analytes. Elution order here is: chlorogenic acid, caffeic acid, luteolin and quercetin.

5.5 Multidimensional Liquid Chromatography with Surface-Enhanced Raman Spectroscopy

After the fractions were collected for the desired analytes, a 5 µL aliquot was drop coated onto the optimised FP substrates in aliquots of 5 µL. The samples were then subjected to SERS analysis; Figure 5.18 shows SERS spectra of the collected fractions of the peaks denoted with asterisks from Figure 5.17. Unfortunately, the SERS signal was very weak and did not detect any presence of analyte on the surface. Only the strong ν(Ag-Cl) mode at 230 cm^{-1} could be detected (resulting from the KCl treatment). The reasoning behind the weak signal was suspected to be sample dilution. Since only 1.0 µL of the 25 ppm mixture was initially injected onto the column, and it is known that through the separation process some dilution will occur, it is feasible to suggest that the fraction collected was too dilute to be detected using the FP substrate. Thus different injection volumes were investigated next in order to identify if a more concentrated sample could be collected during fraction collection, thus improving the chance for a successful SERS analysis.

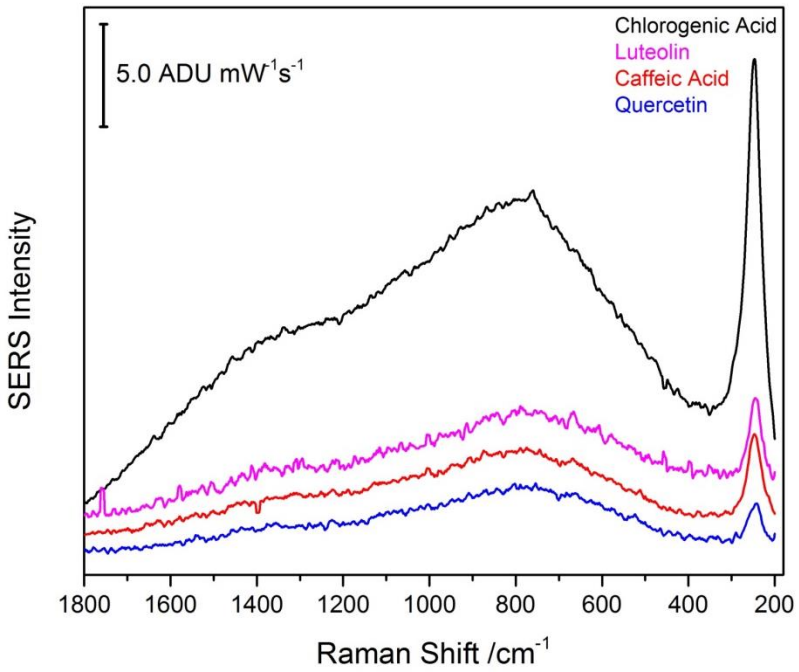

Figure 5.18: SERS spectra of fractions collected from peaks denoted with asterisks from Figure 5.17 (30 s, 12.17 mW, 785 nm laser).

Increased injection volumes of 2.0, 3.0, and 4.0 µL were investigated. Too high of injection volumes were avoided in order to not overload the column. The ^{1}D and the ^{2}D chromatograms are shown in Figures 5.19 and 5.20 respectively. It can be seen that increased injection volumes do correlate to a higher absorbance and more intense peaks. This in turn led to a greater volume collected from each fraction as more of the peak was above the threshold for fraction collection (5 mAU). Despite the greater volumes collected per each increase in injection volume, the SERS did not show a significant improvement. Figure 5.21 shows the SERS signal from chlorogenic acid (the first peak collected from each run) at each of the differing injection volumes as it gave the most intense signal of any fraction. As the injection volume increases it appears that the SERS signal weakens, with even the ν(Ag-Cl) mode decreasing in intensity. This could be due to the increased volume collected in the fractions having the opposite effect as intended.

Instead of collecting a more concentrated sample, the fraction contained a similar amount of sample but much more solvent thus creating an even more dilute fraction than the initial trial. The best SERS signal (injection volume of 4.0 µL) is compared against the 1.0 mM SERS signal of chlorogenic acid for reference in Figure 5.22.

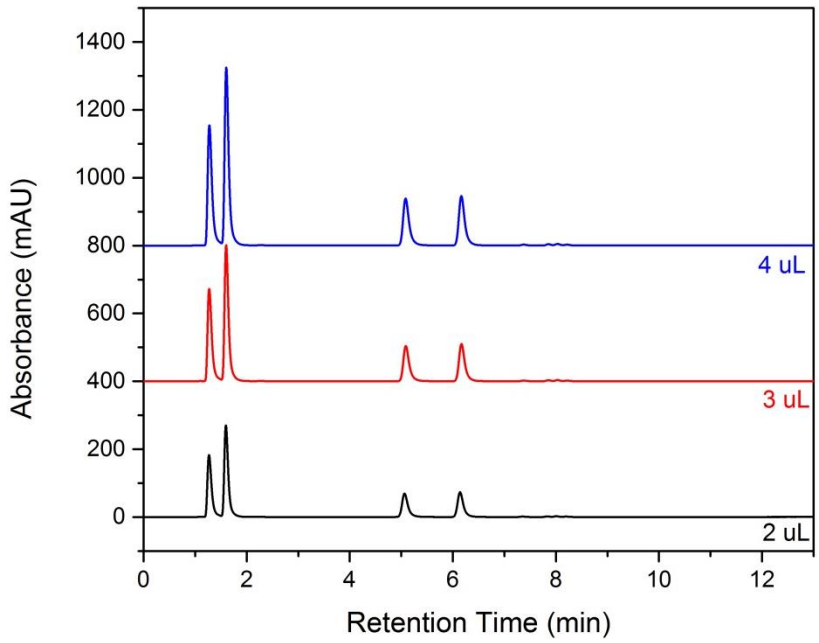

Figure 5.19: [1]D chromatogram of 25 ppm mixture (50:50% v/v, MeOH:H_2O) at 327 nm with injection volumes of 2.0, 3.0, and 4.0 µL. [2]D-threshold of 20 mAU.

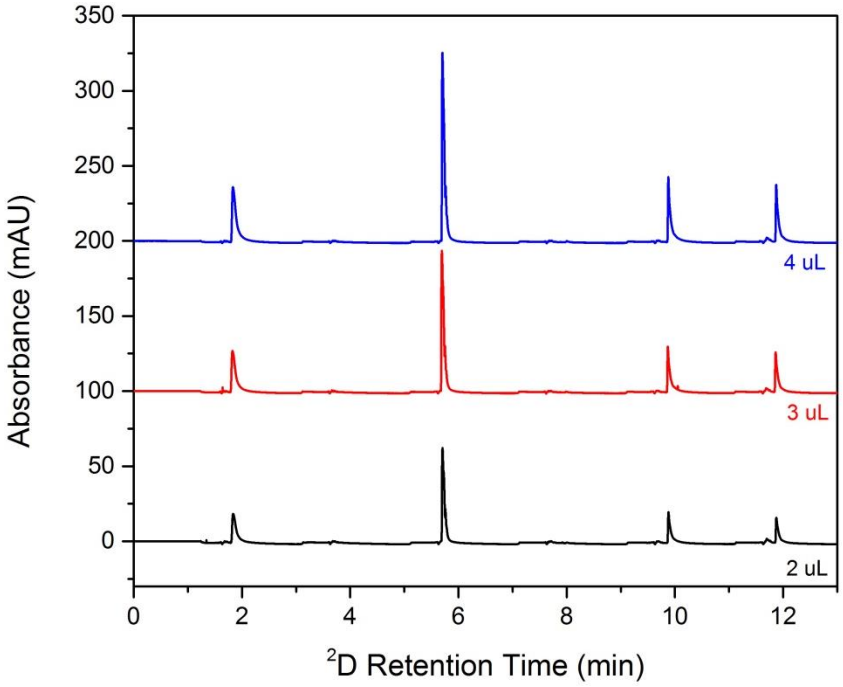

Figure 5.20: ^{2}D chromatogram of 25 ppm mixture (50:50% v/v, MeOH:H_2O) at 327 nm with injection volumes of 2.0, 3.0, and 4.0 µL. Fraction collection threshold of 5.0 mAU.

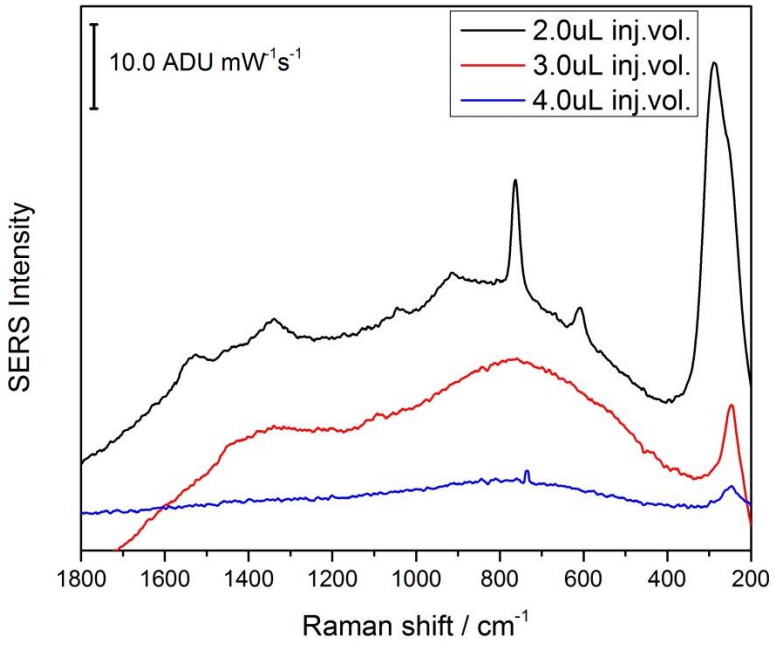

Figure 5.21: SERS spectra of fractions collected from the first peak (chlorogenic acid) of each injection volume from Figure 5.20 (30 s, 12.17 mW, 785 nm laser).

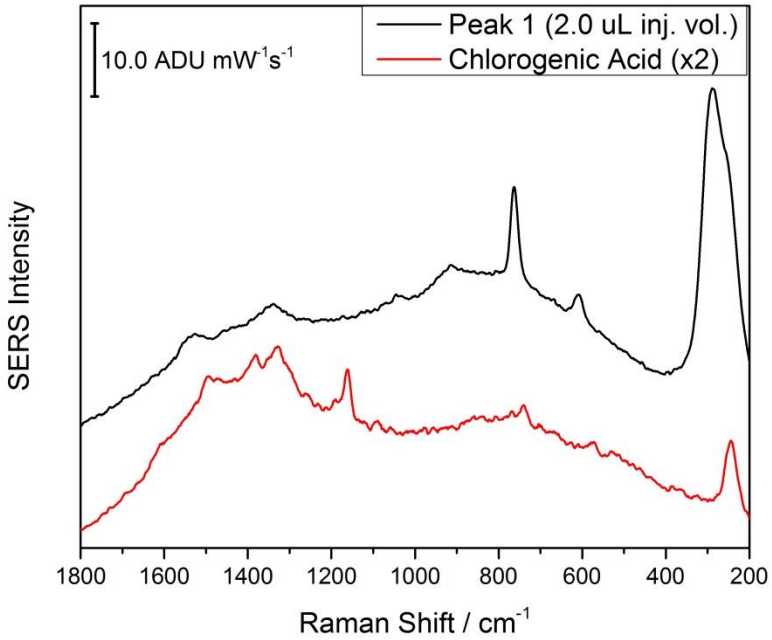

Figure 5.22: SERS spectra of fraction collected for chlorogenic acid using 2.0 µL injection volume from Figure 5.20 compared to 1.0 mM chlorogenic acid (30 s, 12.17 mW, 785 nm laser).

It is clear that there is still a discrepancy between the SERS signal of the fractions collected after the chromatographic process and the achievable signal for 50 ppm solutions of each standard separately (Figure 5.12) and the 25 ppm mixture before injection to the instrument (Figure 5.23). In order to assess the dilution of the fractions, each fraction was examined using UV-vis spectroscopy (Figure 5.24). Their intensities are comparable to that of the 25 ppm mixture diluted by a factor of 10 (Figure 5.13). Thus it can be interpreted that the final concentration of the fractions after being separated by two dimensions is approximately 2.5 ppm. This is therefore below the limit of detection for the optimized FP SERS substrates and thus a more concentrated sample, ex: 500 ppm, would be needed in order to obtain fractions that are more concentrated and have shown to be achievable by the FP substrates, ex. 50 ppm.

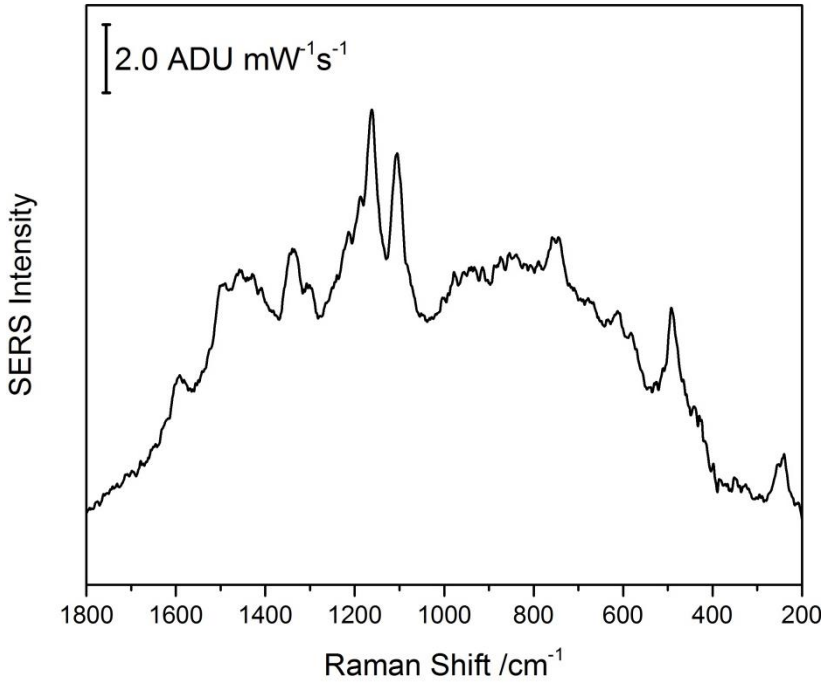

Figure 5.23: SERS of 25 ppm mixture of luteolin, quercetin, chlorogenic acid, and caffeic acid in MeOH:H_2O (50:50 % v/v) on optimized FP SERS substrate (30 s, 12.17 mW, 785 nm laser).

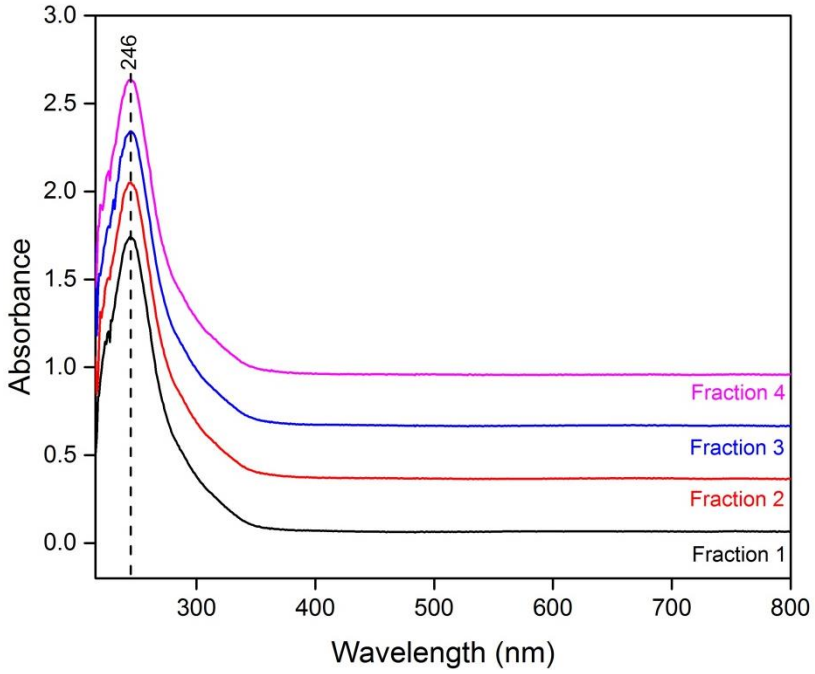

Figure 5.24: UV-vis absorbance spectra of fractions 1-4 obtained after 2D-LC separation of the 25 ppm mixture of polyphenolic standards.

5.6 Discussion

This thesis successfully created an optimized 3D SERS substrate for the detection of polyphenolic compounds. Filter paper (FP) was used as a more sustainable and cost-effective alternative to conventional 2D substrates and proved to provide consistent and reliable data. Signal, however, was only obtained using FP substrates once a series of surface treatments were performed. A KCl treatment was used to displace citrate ions from the nanoparticle surface. This allows the analyte closer access to the surface and thus it could benefit from the SERS enhancement. A surface treatment technique using pyridine (pyr) was also shown to be vital for the detection of polyphenols. Through EC-SERS investigations, pyr was discovered to be present in a planar orientation to the surface. This is an important discovery as it provides an explanation for the analyte SERS enhancement observed when pyr is present. In a planar orientation, both the lone pair of electrons on the nitrogen atom and the double bond nature of the pyridine ring are able to interact with the analyte molecules and draw them closer to the surface due to hydrogen bonding and van der Waals interactions respectively. The optimised FP SERS substrate was able to detect concentrations of pure polyphenolic compounds down to 50 ppm, and a mixture of 4 (luteolin, quercetin, chlorogenic acid, and caffeic acid) down to a concentration of 25 ppm.

Optimised methodologies were developed for both 1D and 2D-LC separation of a simple polyphenolic mixture. After separation in the ^{2}D, fractions of the separated components were collected and subsequently analysed using SERS. It is important to highlight that this offline SERS detection for 2D-LC technique is the first of its kind performed. Despite showing great promise, the SERS detection yielded no useful signal. It was theorised that the final concentration of the fractions was too dilute to be measured

using the FP SERS substrates, thus several optimisation strategy were attempted in effort to increase the final fraction concentration. These attempts did not yield the desired outcome, therefore UV-vis spectroscopy was utilised to test the final concentration of the fractions. The fractions collected after the separation by 2D-LC were approximately 2.5 ppm and therefore too dilute to be detected using the FP SERS substrates. This indicates that future work should focus on either more concentrated fractions or more sensitive SERS substrates.

Chapter 6: Conclusions and Future Work

6.1 Conclusions

This thesis work successfully optimized filter paper (FP) substrates for the surface-enhanced Raman spectroscopy (SERS) detection of polyphenolic compounds. This included the surface treatments with potassium chloride (KCl) and pyridine (pyr) solutions. KCl was able to displace citrate from the surface to have enhanced SERS signal of analytes. Pyr functionalization proved to be essential to the SERS substrates but its role was previously unknown. Through electrochemical SERS (EC-SERS) measurements to manipulate the molecular orientation, it was discovered that pyr assumes a planar orientation on the surface with no applied potential, and only once a negative potential was applied did it adopt a perpendicular arrangement on the surface. This provided insight on the surface functionalization as the polyphenolic compounds would be drawn to the substrate surface through strong van der Waals interactions and thus be able to benefit from the SERS enhancement. In a sense, the pyr layer acts as a "carpet" for the polyphenols to adsorb onto. As a result, this thesis work provides a new strategy for efficient SERS detection of polyphenols and offers insight into the most likely reason for improved SERS signal using this strategy.

This thesis work was also the first known attempt to combine multidimensional liquid chromatography with surface-enhanced Raman spectroscopy (2D-LC-SERS) as an offline detector for phenolic acids. An optimised 2D-LC method was created for the separation of polyphenols, and this method successfully separated mixtures of four polyphenolic compounds in multiple dimensions and fractions were able to be collected. After a second dimension separation, SERS was applied as an offline characterization tool by depositing the collected fractions onto the FP substrates. Detection of a SERS

signal for the polyphenols proved to be challenging and several strategies to try and enhance the signal were explored. This included increasing the volume of standard injected onto the column, and exploring the extent to which the sample was being diluted throughout the chromatographic process. Although no identifiable SERS signal was able to be obtained, this work shows promise for future endeavours into this novel coupling of chromatographic and spectroscopic techniques.

6.2 Future Work

In the future, more trials of the 2D-LC-SERS detection need to be completed. A more concentrated mixture of 500 ppm should also be separated to determine if the lack of SERS signal is indeed due to the diluted nature of the collected fractions. In addition, it has been noted in literature that LC methods that use acetonitrile may mask the SERS signal[58]; therefore another option would be to replace the second dimension mobile phase B with an alternate solvent. SERS signal of fractions collected from any new method can then be compared to the results in this thesis work.

Once a clear and reproducible approach for 2D-LC-SERS has been found, it should be applied to real world samples. Natural extracts that are high in polyphenolic content such as green tea, berries, and wines extracts could be separated with 2D-LC-SERS and compared to literature values to aid in the discovery of new compounds and expand literature on the exacts components of the extracts. In addition, creation of a spectral library of known polyphenolic compounds would be helpful for the rapid identification of unknown substances in the natural extracts.

References

(1) Stoll, D. R.; Carr, P. W. *Anal. Chem.* **2017**, *89* (1), 519–531.

(2) Carr, P. W.; Stoll, D. R. *Agil. Tech. Note* **2015**, 1–163.

(3) Donovan, J. L.; Manach, C.; Faulks, R. M.; Kroon, P. A. Crozier, A., Clifford, M. N., Ashihara, H., Eds.; Blackwell Publishing: Oxford, 2006; p 372.

(4) Merken, H. M.; Beecher, G. R. *J. Agric. Food Chem.* **2000**, *48* (3), 577–599.

(5) Kittlaus, S.; Schimanke, J.; Kempe, G.; Speer, K. *J. Chromatogr. A* **2013**, *1283*, 98–109.

(6) Qiu, S.; Yang, W. Z.; Shi, X. J.; Yao, C. L.; Yang, M.; Liu, X.; Jiang, B. H.; Wu, W. Y.; Guo, D. A. *Anal. Chim. Acta* **2015**, *893*, 65–76.

(7) Wang, J.; Xu, Y.; Wen, C.; Wang, Z. *Anal. Chim. Acta* **2017**, *992*, 42–54.

(8) Cowcher, D. P.; Jarvis, R.; Goodacre, R. *Anal. Chem.* **2014**, *86* (19), 9977–9984.

(9) Nguyen, A. H.; Deutsch, J. M.; Xiao, L.; Schultz, Z. D. *Anal. Chem*. **2018**, 11062–11069.

(10) Editorial. *Nat. Chem. Biol.* **2007**, *3* (7), 351.

(11) Crozier, A.; Jaganath, I.; Clifford, M. *Phenols, Polyphenols and Tannins: An Overview*; 2007.

(12) Diaconeasa, Z.; Florica, R.; Rugina, D.; Lucian, C.; Socaciu, C. *J. Food Nutr. Res.* **2014**, *2* (11), 781–785.

(13) Panche, A. N.; Diwan, A. D.; Chandra, S. R. *J. Nutr. Sci.* **2016**, *5*.

(14) Mandal, S. M.; Chakraborty, D. In *Natural Products: Phytochemistry, Botany and Metabolism of Alkaloids, Phenolics and Terpenes*; Ramawat, K. G., Mérillon, J.-M., Eds.; Springer Berlin Heidelberg: Berlin, Heidelberg, 2013; pp 2047–2059.

(15) Choi, J. M.; Hahm, E.; Park, K.; Jeong, D.; Rho, W.-Y.; Kim, J.; Jeong, D. H.; Lee,

Y.-S.; Jhang, S. H.; Chung, H. J.; Cho, E.; Yu, J.-H.; Jun, B.-H.; Jung, S. *Nanomaterials* **2017**, *7*, 8.

(16) Rao, Y.; Zhao, X.; Li, Z.; Huang, J. *Talanta* **2018**, *190*, 174–181.

(17) Jurasekova, Z.; Domingo, C.; Garcia-Ramos, J. V; Sanchez-Cortes, S. *J. Raman Spectrosc.* **2012**, *43* (12), 1913–1919.

(18) Hu, C.; Kitts, D. D. *J. Agric. Food Chem.* **2003**, *51* (1), 301–310.

(19) Crozier, A.; Yokota, T.; Jaganath, I. B.; Marks, S.; Saltmarsh, M.; Clifford, M. N. Secondary Metabolites in Fruits, Vegetables, Beverages and Other Plant-based Dietary Components In *Plant Secondary Metabolites*; Crozier, A., Clifford, M.N., Ashihara, H., Ed.; Blackwell: Oxford, 2006; pp 208-302.

(20) Hernández-Borges, J.; González-Hernández, G.; Borges-Miquel, T.; Rodríguez-Delgado, M. A. *Food Chem.* **2005**, *91* (1), 105–111.

(21) Hasegawa, S.; Berhow, M. A.; Fong, C. H. In *Fruit Analysis*; Linskens, H. F., Jackson, J. F., Eds.; Springer: Berlin, Heidelberg, 1995; pp 59–80.

(22) Dolowy, M.; Pyka, A. *Biomed. Chromatogr.* **2014**, *28* (1), 84–101.

(23) Beni, Á.; Lajtha, K.; Kozma, J.; Fekete, I. *J. Microbiol. Methods* **2017**, *136*, 1–5.

(24) Thieme, D.; Sachs, H. *Anal. Chim. Acta* **2003**, *492* (1–2), 171–186.

(25) Nováková, L.; Matysová, L.; Solich, P. *Talanta* **2006**, *68* (3), 908–918.

(26) *HPLC in Nucleic Acid Research: Methods and Applications*; Brown, P. R., Ed.; Marcel Dekker, INC.: New York, 1984.

(27) McMaster, M. C. *HPLC: A Practical User's Guide*, 2nd ed.; John Wiley & Sons, Inc.: Hoboken, New Jersey, 2007.

(28) Guillarme, D.; Veuthey, J. L. *UHPLC in Life Sciences*; RSC Chromatography Monographs; Royal Society of Chemistry, 2015.

(29) Skoog, D. A.; West, D. M.; Holler, F. J.; Crouch, Stanley, R. *Fundamentals of Analytical Chemistry*; Brooks/Cole Cengage learning: Belmont, CA, 2004; pp 973–995.

(30) De Villiers, A.; Venter, P.; Pasch, H. *J. Chromatogr. A* **2015**, *1430*, 16–78.

(31) Martínez-Cruz, O.; Paredes-López, O. *J. Chromatogr. A* **2014**, *1346*, *43-48*.

(32) Andreu-Navarro, A.; Fernández-Romero, J. M.; Gómez-Hens, A. *J. Sep. Sci.* **2010**, *33* (4-5), 509–515.

(33) Kalili, K. M.; De Villiers, A. *J. Sep. Sci.* **2010**, *33* (6-7), 853–863.

(34) Biesaga, M.; Ochnik, U.; Pyrzynska, K. *J. Sep. Sci.* **2009**, *32* (15-16), 2835–2840.

(35) Silva, C. L.; Pereira, J.; Wouter, V. G.; Giró, C.; Câmara, J. S. *Talanta* **2011**, *86* (1), 82–90.

(36) Aznar, O.; Checa, A.; Oliver, R.; Hernandez-Cassou, S.; Saurina, J. *J. Sep. Sci.* **2011**, *34* (5), 527–535.

(37) Qiao, X.; Song, W.; Ji, S.; Wang, Q.; Guo, D.; Ye, M. *J. Chromatogr. A* **2015**, *1402*, 36–45.

(38) Giddings, J. C. *J. High Resolut. Chromatogr.* **1987**, *10*, 319–323.

(39) Davis, J. M.; Giddings, J. C. *Anal. Chem.* **1983**, *55* (3), 418–424.

(40) Giddings, J. C. *Anal. Chem.* **1984**, *56* (12), 1258A–1270A.

(41) Li, Z.; Chen, K.; Guo, M.; Tang, D. *J. Sep. Sci.* **2016**, *39* (1), 21–37.

(42) Pierce, K. M.; Kehimkar, B.; Marney, L. C.; Hoggard, J. C.; Synovec, R. E. *J. Chromatogr. A* **2012**, *1255*, 3–11.

(43) Whitworth, R. *Anal. Sci. Agil. Technol.* **2014**, 1–26.

(44) Scoparo, C. T.; de Souza, L. M.; Dartora, N.; Sassaki, G. L.; Gorin, P. A. J.;

Iacomini, M. *J. Chromatogr. A* **2012**, 1222, 29-37.

(45) Kalili, K. M.; Vestner, J.; Stander, M. A.; de Villiers, A. *Anal. Chem.* **2013**, *85* (19), 9107-9115.

(46) Qiao, X.; Song, W.; Ji, S.; Li, Y.-J.; Wang, Y.; Li, R.; An, R.; Guo, D.; Ye, M. *J. Chromatogr. A* **2014**, *1362*, 157–167.

(47) Jeanmaire, D. L.; Van Duyne, R. P. *J. Electroanal. Chem. Interfacial Electrochem.* **1977**, *84* (1), 1–20.

(48) Fleischmann, M.; Hendra, P. J.; McQuillan, A. J. *Chem. Phys. Lett.* **1974**, *26* (2), 163–166.

(49) Creighton, J. A.; Albrecht, M. G.; Hester, R. E.; Matthew, J. A. D. *Chem. Phys. Lett.* **1978**, *55* (1), 55–58.

(50) Cañamares, M. V.; Reagan, D. A.; Lombardi, J. R.; Leona, M. *J. Raman Spectrosc.* **2014**, *45* (11–12), 1147–1152.

(51) Willets, K. A.; Duyne, R. P. Van. *Annu. Rev. Phys. Chem.* **2007**, *58*, 267–297.

(52) Heaps, D. A.; Griffiths, P. R. *Appl. Spectrosc.* **2005**, *59* (11), 1305–1309.

(53) Zhu, Q.; Cao, Y.; Cao, Y.; Chai, Y.; Lu, F. *Anal. Bioanal. Chem.* **2014**, *406* (7), 1877–1884.

(54) Huang, R.; Han, S.; Li, X. S. *Anal. Bioanal. Chem.* **2013**, *405* (21), 6815-6822.

(55) Carron, K.; Kennedy, B. *Anal. Chem.* **1995**, *67* (18), 3353–3356.

(56) Roth, E.; Kiefer, W. *Appl. Spectrosc.* **1994**, *48*, 1193–1195.

(57) Riordan, C. M.; Jacobs, K. T.; Negri, P.; Schultz, Z. D. *Faraday Discuss.* **2016**, *187*, 473–484.

(58) Trachta, G.; Schwarze, B.; Sägmüller, B.; Brehm, G.; Schneider, S. *J. Mol. Struct.* **2004**, *693* (1–3), 175–185.

(59) Zhang, L.; Zhou, L.; Ji, W.; Song, W.; Zhao, S. *Food Anal. Methods* **2017**, *10* (6), 1940–1947.

(60) Lee, C. H.; Hankus, M. E.; Tian, L.; Pellegrino, P. M.; Singamaneni, S. *Anal. Chem.* **2011**, *83* (23), 8953–8958.

(61) Wang, C.; Liu, B.; Dou, X. *Sensors Actuators B Chem.* **2016**, *231*, 357–364.

(62) Kleinman, S. L.; Frontiera, R. R.; Henry, A. I.; Dieringer, J. A.; Van Duyne, R. P. *Phys. Chem. Chem. Phys.* **2013**, *15* (1), 21–36.

(63) Meyer, V. R. *Practical High-Performance Liquid Chromatography*, Fourth.; John Wiley & Sons, Inc.: Hoboken, New Jersey, 2004.

(64) Manz, A.; Dittrich, P. S.; Pamme, N.; Iossifidis, D. *Bioanalytical Chemistry: Second Edition*; Imperial College Press, 2015.

(65) Stoll, D. R. In *Handbook of Advanced Chromatography/Mass Spectrometry Techniques*; Holcapek, M., Byrdwell, W. C., Eds.; Academic Press and AOCS Press: London, 2017; pp 227–286.

(66) Wei, A. In *Nanoparticles: Building Blocks for Nanotechnology*; Rotello, V., Ed.; Kluwer Academic/ Plenum Publishers: New York, 2011; pp 173–200.

(67) Rycenga, M.; Cobley, C. M.; Zeng, J.; Li, W.; Moran, C. H.; Zhang, Q.; Qin, D.; Xia, Y. *Chem. Rev.* **2011**, *111* (6), 3669–3712.

(68) Kelly, K. L.; Coronado, E.; Zhao, L. L.; Schatz, G. C. *J. Phys. Chem. B* **2003**, *107* (3), 668–677.

(69) Ferraro, J. R.; Nakamoto, K. *Introductory Raman Spectroscopy*; Academic Press, Inc.: San Diego, 1994.

(70) Pelletier, M. J. *Analytical Applications of Raman Spectroscopy*; Pelletier, M. J., Ed.; Blackwell Science Ltd.: Oxford, 1999.

(71) Bantz, K. C.; Meyer, A. F.; Wittenberg, N. J.; Im, H.; Kurtulus, O.; Lee, S. H.; Lindquist, N. C.; Oh, S.-H.; Haynes, C. L. **2011**, *13* (24), 11551–11567.

(72) Kneipp, K.; Kneipp, H.; Itzkan, I.; Dasari, R. R.; Feld, M. S. *J. Physics-Condensed Matter* **2002**, *14* (18), R597–R624.

(73) Kennedy, B. J.; Spaeth, S.; Dickey, M.; Carron, K. T. *J. Phys. Chem. B* **1999**, *103* (18), 3640–3646.

(74) Wang, J. *Analytical Electrochemistry*, 2nd ed.; Wiley-VCH: New York, 2000.

(75) Bard, A. J.; Faulkner, L. R. *Electrochemical methods: Fundamentals and applications*, 2nd ed.; John Wiley & Sons, Inc.: New York, 2001.

(76) Zhao, L.; Blackburn, J.; Brosseau, C. L. *Anal. Chem.* **2015**, *87* (1), 441–447.

(77) Greene, B. H. C.; Alhatab, D. S.; Pye, C. C.; Brosseau, C. L. *J. Phys. Chem. C* **2017**, *121* (14), 8084–8090.

(78) Lynk, T. P.; Clarke, O. J. R.; Kesavan, N.; Brosseau, C. L. *Sensors Actuators B Chem.* **2018**, *257*, 270–277.

(79) De Bleye, C.; Dumont, E.; Hubert, C.; Sacré, P. Y.; Netchacovitch, L.; Chavez, P. F.; Hubert, P.; Ziemons, E. *Anal. Chim. Acta* **2015**, *888*, 118–125.

(80) Alstrom. Laboratory products catalog. 2016, p 28.

(81) Pan, T.; Sun, D.-W.; Pu, H.; Wei, Q. *J. Agric. Food Chem.* **2018**, *66* (9), 2180–2187.

(82) Saito, H. *Bull. Chem. Soc. Jpn.* **1993**, *66* (3), 963–965.

(83) Jeanmaire, D. L.; Van Duyne, R. P. *Journal of Electroanalytical Chemistry and Interfacial Electrochemistry*. 1977, pp 1–20.

(84) Greenler, R. G.; Snider, D. R.; Witt, D.; Sorbello, R. S. *Surf. Sci.* **1982**, *118* (3), 415–428.

(85) Moskovits, M.; Suh, J. S. *J. Phys. Chem.* **1984**, *88* (23), 5526–5530.

(86) Sun, S. C.; Bernard, I.; Birke, R. L.; Lombardi, J. R. *J. Electroanal. Chem. Interfacial Electrochem.* **1985**, *196* (2), 359–374.

(87) Jurasekova, Z.; Torreggiani, A.; Tamba, M.; Sanchez-Cortes, S.; Garcia-Ramos, J. V. *J. Mol. Struct.* **2009**, *918* (1–3), 129–137.

(88) Sánchez-Cortés, S.; García-Ramos, J. V. *Appl. Spectrosc.* **2000**, *54* (2), 230–238.

(89) Jurasekova, Z.; Garcia-Ramos, J. V; Domingo, C.; Sanchez-Cortes, S. *J. Raman Spectrosc.* **2006**, *37* (11), 1239–1241.

(90) Maiti, N.; Kapoor, S.; Mukherjee, T. *Adv. Mater. Lett.* **2013**, *4* (6), 502–506.

Appendix

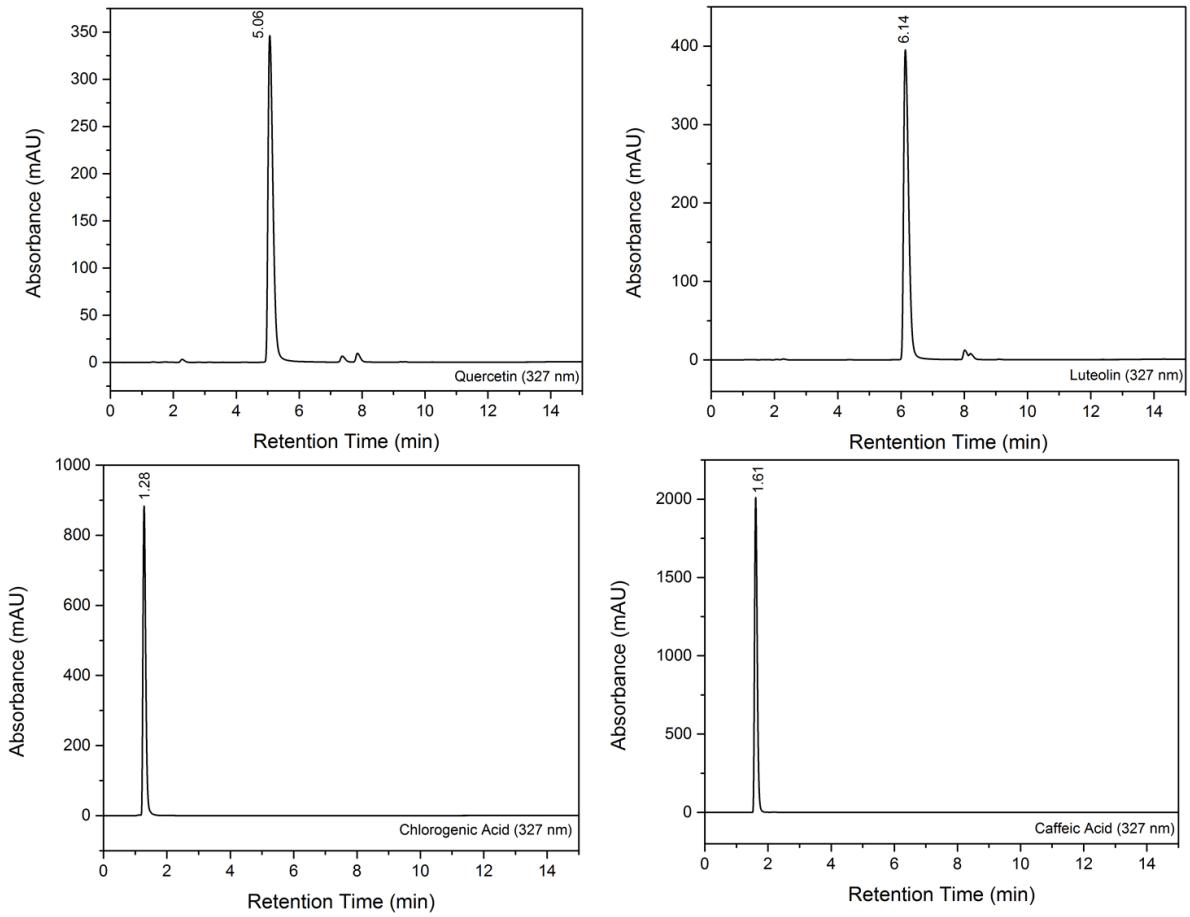

Figure A.1: [1]D chromatograms for 100 ppm (50:50% v/v, MeOH:H_2O) solutions of luteolin, quercetin, chlorogenic acid, and caffeic acid at 327 nm with retention times stated above each main peak.

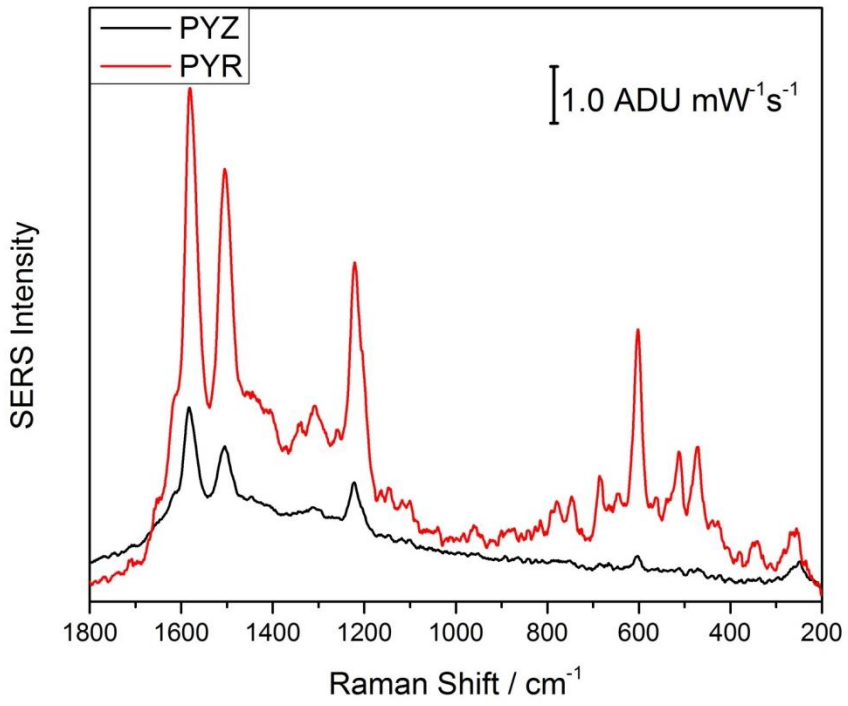

Figure A.2: SERS spectra of 1.0 mM luteolin on KCl treated FP substrates using pyr (red) and pyz (black) as surface functionalization molecules.